

# An analytical approach to codimension-2 sliding bifurcations in the dry friction oscillator

M. Guardia\*, S. J. Hogan†, T. M. Seara‡

July 31, 2009

\*‡ Departament de Matemàtica Aplicada I  
Universitat Politècnica de Catalunya  
Diagonal 647, 08028 Barcelona, Spain

† Department of Engineering Mathematics  
University of Bristol  
Queen's Building, University Walk, BS8 1TR Bristol, United Kingdom

## Abstract

In this paper, we consider analytically sliding bifurcations of periodic orbits in the dry friction oscillator. The system depends on two parameters;  $F$ , which corresponds to the intensity of the friction and  $\omega$ , the frequency of the forcing. We prove the existence of infinitely many codimension-2 bifurcation points and we focus our attention on two of them;  $A_1 := (\omega^{-1}, F) = (2, 1/3)$  and  $B_1 := (\omega^{-1}, F) = (3, 0)$ . We derive analytic expressions in  $(\omega^{-1}, F)$  parameter space for the codimension-1 bifurcation curves that emanate from  $A_1$  and  $B_1$ . We show excellent agreement with the numerical calculations of Kowalczyk and Piiroinen [KP08].

Keywords: Filippov systems, periodic orbits, sliding bifurcations, codimension-2 points.

AMS classification scheme numbers: 37G15, 34A36, 34C25, 34C23.

## 1 Introduction

### 1.1 Preliminaries

The study of nonsmooth (or piecewise smooth) dynamical systems has gained considerable ground in recent years. These systems are interesting for two reasons; firstly they behave in ways that are distinct from smooth systems and secondly they are found in many important application areas. For example,

---

\*marcel.guardia@upc.edu

†S.J.Hogan@bristol.ac.uk

‡tere.m-seara@upc.edu

DC/DC power converters [BV01, FHS09], impacting systems [Nor91], hybrid dynamical systems [BH03], systems with backlash or free-play [BN99] and mechanical systems with friction [OHP95, BG00] are all examples of nonsmooth systems. The recent book [dBCK08] gives an excellent introduction to the subject.

Nonsmooth systems differ from smooth systems in the way bifurcations can occur. The study of local bifurcations has been done by many authors either numerically or analytically for discontinuous maps and flows [KRG03, AS06, BPS01, Tei81, Tei90, Tei93, Tei99, SM07, SM08, SM09], but this is not the subject of this paper.

Global nonsmooth bifurcations can happen when the system  $\Omega$ -limit set, for instance a limit cycle, collides with a system *switching manifold* (a hyperplane in phase space across which the system dynamics varies nonsmoothly). Up to now, the global bifurcations of periodic orbits have been studied either using the zero discontinuity map [Nor91, FN97, Nor02] or by numerical continuation methods [KP08, DK05]. In this paper we present a more classical constructive approach which allows us to rigorously prove the existence of some of these bifurcations in a specific model. This is possible in our model for two reasons: the system is piecewise linear and we can explicitly construct pieces of periodic orbits as they visit the different regions of the phase space. Nevertheless, gluing these pieces together is not an easy analytical problem, since it involves solving transcendental equations. However construction is made easier because when the periodic orbit undergoes a nonsmooth bifurcation it has to contain some specific points in the switching manifold.

When the vector field either side of a switching manifold points toward the manifold, then it is possible for the system trajectory to be restricted to that part of the switching manifold known as the *sliding region*. A *sliding bifurcation* occurs when, under parameter variation, a trajectory in the  $\Omega$ -limit set no longer enters the sliding region. These bifurcations are summarized in [Fil88]. See also the excellent introduction in [KP08] for a detailed account of these bifurcations in the case of periodic orbits.

The dry friction oscillator is a very good example of a nonsmooth system containing sliding bifurcations of periodic orbits. It is a system of great engineering importance and has been the subject of intense study for many years; from analytical, numerical and experimental points of view (see [Dan99, Har31, WSWK08]).

A mass sits on a rough table. It is connected to a fixed wall via a spring and is excited sinusoidally. In the simplest manifestation of the problem, the friction is modeled by Coulomb's law (see [Cou85]), that is, friction is assumed to be constant and opposed to the relative velocity between the mass and the table. In this case, the mass can undergo three different types of motion; *stick*, *slip* and *stick-slip*. In the first type of motion, the mass never moves because the amplitude of the driving force is insufficient to overcome the frictional force between the mass and the table. In the second case, friction is not strong enough to make the block stop. It is the third case that concerns us here, where the mass sticks to the table with zero velocity (thus defining the sliding region) for some non-zero time interval less than the period of oscillation of the table. Note that this leads to an unavoidable linguistic ambiguity; physically the mass *sticks* to the table, yet mathematically it is said to be *sliding*.

The assumption of Coulomb friction leads to a system with two parameters  $\omega$  and  $F$  which refer to the frequency of the sinusoidal forcing and the strength of the friction respectively. Thus, one can study the nonsmooth sliding bifurcations that the system can undergo when these two parameters are varied.

The codimension-2 bifurcation points organize the  $(\omega^{-1}, F)$  bifurcation diagram. Further work [KdB05] has shown that no smooth bifurcations can merge with these nonsmooth codimension-2 points. For this to happen, it is necessary to consider a more sophisticated friction law (see [NK06]).

With a suitable scaling, the dry-friction oscillator with Coulomb friction can be described by the following equation:

$$\ddot{x} = -x + \sin(\omega t) - F \operatorname{sgn}(\dot{x}), \quad (1)$$

where the sign function is given by

$$\operatorname{sgn}(z) = \begin{cases} 1 & \text{if } z > 0 \\ -1 & \text{if } z < 0. \end{cases} \quad (2)$$

In this paper, we will study analytically the existence, behaviour and bifurcations of periodic orbits of equation (1).

The dry-friction oscillator has been studied widely numerically. Early work in this area [Fei94] showed that there is a number of bifurcations in  $(\omega^{-1}, F)$  parameter space and numerical evidence was presented of nonsmooth codimension-2 bifurcations at the intersection of codimension-1 bifurcation curves (see also [KdB05]). In particular the phase space topology around the codimension-2 sliding bifurcation point  $(\omega^{-1}, F) = (2, 1/3)$  was partially determined analytically. In [KdBC<sup>+</sup>06] and [KP08], a unique  $2\pi/\omega$ -periodic orbit, whose existence was proved by Kunze in [Kun00] (see Section 1.4), was numerically found in a certain range of the parameters. Then, using numerical continuation, sliding bifurcations of the limit cycle were detected.

The main goal of the present paper is to study analytically this periodic orbit and to determine locally its codimension-1 bifurcation curves in  $(\omega^{-1}, F)$  parameter space. We prove rigorously the existence of an infinite number of two types of codimension-2 bifurcation points  $A_n, B_n$ . The points  $A_n$  are classical codimension-2 nonsmooth bifurcations where the periodic orbit grazes on a cusp of the discontinuity surface. The points  $B_n$  are bifurcation points that occur in the “limiting” smooth system without friction. We also give implicit analytic expressions for several codimension-1 curves through the points  $A_n$  and we give some asymptotic expansions of these curves at  $A_1$ , which was numerically studied in [KP08]. In particular, we show that the behaviour encountered numerically in  $A_1$  in that paper is a universal behaviour in any point  $A_n$ . Concerning the second set of bifurcation points  $B_n$ , we focus our attention on  $B_1$  and we give local asymptotic expansions for several codimension-1 bifurcation curves through it.

$A_n, B_n$  are not the only codimension-2 bifurcation points of this system. In fact, in [KP08], the authors detected numerically several more codimension-2 bifurcation points in certain range of the parameters, and moreover, the whole bifurcation diagram is far from being completely understood.

## 1.2 The dry-friction oscillator as a Filippov System

Rewriting the non-autonomous equation (1) as a first order autonomous system, we obtain

$$\begin{cases} \dot{x} = y \\ \dot{y} = -x + \sin(s) - F \operatorname{sgn}(y) \\ \dot{s} = \omega \end{cases} \quad (3)$$

which can be written as  $\dot{z} = X(z)$ , where  $z = (x, y, s)$  is defined in  $\mathbb{R}^2 \times \mathbb{T}^1$ , where  $\mathbb{T}^1 = \mathbb{R}/2\pi\mathbb{Z}$ .

This system is continuous and even analytic in

$$\begin{aligned} G_1 &= \{(x, y, s) \in \mathbb{R}^2 \times \mathbb{T}^1, y > 0\} \\ G_2 &= \{(x, y, s) \in \mathbb{R}^2 \times \mathbb{T}^1, y < 0\}. \end{aligned} \quad (4)$$

It has a unique surface of discontinuity

$$\Sigma = \{(x, y, s) \in \mathbb{R}^2 \times \mathbb{T}^1, f(x, y, s) = 0\} \quad \text{where } f(x, y, s) = y. \quad (5)$$

Mathematically,  $\Sigma$  is the switching manifold; physically it corresponds to zero velocity. We denote the vector field defined in  $G_1$  as  $X_1$  and the vector field defined in  $G_2$  as  $X_2$ .

The switching manifold  $\Sigma$  can be split into three regions (see Figure 1):

1. Crossing region pointing upwards:  $\Sigma_c^+ = \{(x, y, s) \in \mathbb{R}^2 \times \mathbb{T}^1, y = 0, x < -F + \sin s\}$  where the vector field points away from  $\Sigma$  in  $G_1$  and toward  $\Sigma$  in  $G_2$ .
2. Sliding region:  $\Sigma_s = \{(x, y, s) \in \mathbb{R}^2 \times \mathbb{T}^1, y = 0, -F + \sin s < x < F + \sin s\}$  where the vector field points toward  $\Sigma_s$  in both  $G_1$  and  $G_2$ .
3. Crossing region pointing downwards:  $\Sigma_c^- = \{(x, y, s) \in \mathbb{R}^2 \times \mathbb{T}^1, y = 0, F + \sin s < x\}$  where the vector field points toward  $\Sigma$  in  $G_1$  and away from  $\Sigma$  in  $G_2$ .

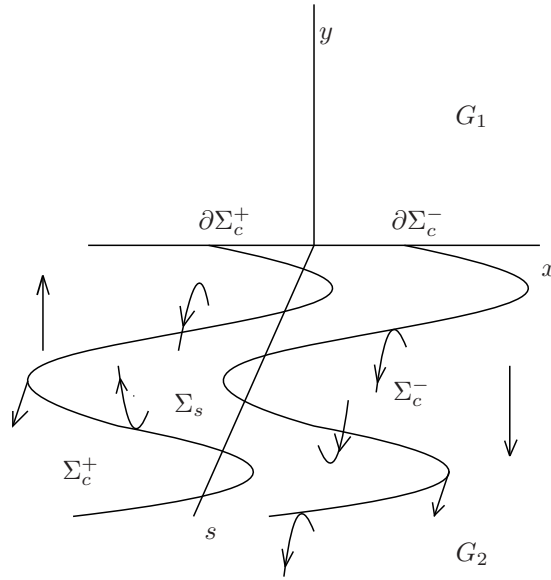


Figure 1: Phase space of system (3).

In  $\Sigma_s$  both vector fields point toward the discontinuity surface. Thus, following Filippov's convex method [Fil88], also called Utkin's *equivalent control* method [Utk92], the dynamics of (3) in this region is given by the sliding vector field, that, in this case, is given by [KP08]:

$$X_s(x, 0, s) = (0, 0, \omega). \quad (6)$$

Physically, in the model of the dry friction oscillator, sliding corresponds to the *absence* of motion in the oscillator due to friction as it is clear from (6). In fact, one of the main challenges in the study of this system is to ascertain whether certain trajectories (for instance the periodic orbit) slip or stick-slip.

We also consider  $\partial\Sigma_c^+$  and  $\partial\Sigma_c^-$  as the boundaries between  $\Sigma_c^+$  and  $\Sigma_s$  and  $\Sigma_s$  and  $\Sigma_c^-$  respectively. These boundaries correspond to tangential contact between  $\Sigma$  and  $X_1$  or  $X_2$ . In system (3), these sets are defined as

$$\begin{aligned}\partial\Sigma_c^+ &= \{(x, y, s) \in \mathbb{R}^2 \times \mathbb{T}^1, f(x, y, s) = 0, X_1 f(x, y, s) = 0\} = \{y = 0, x = -F + \sin s\} \\ \partial\Sigma_c^- &= \{(x, y, s) \in \mathbb{R}^2 \times \mathbb{T}^1, f(x, y, s) = 0, X_2 f(x, y, s) = 0\} = \{y = 0, x = F + \sin s\}\end{aligned}$$

where  $X_i f(p)$  is the Lie derivative of  $f$  with respect to the vector field  $X_i$  in  $p$ . The dynamics around any point  $p \in \partial\Sigma_c^\pm$  is significantly distinct, depending on the kind of tangency at that point. Generically, the tangencies in  $\partial\Sigma_c^\pm$  are quadratic. They are called *folds* in [Tei93] and are the points  $p \in \partial\Sigma_c^\pm$  where  $X_i f(p) = 0$  and  $X_i^2 f(p) \neq 0$ . In [KRG03] they are classified as visible and invisible tangencies depending on the sign of  $X_i^2 f(p)$  (see Figure 1). In system (3), the points  $(x, y, s) \in \partial\Sigma_c^+$  are visible quadratic tangencies of  $X_1$ , provided  $s \in (0, \pi/2) \cup (3\pi/2, 2\pi) \subset \mathbb{T}^1$  and invisible quadratic tangencies of  $X_1$ , provided  $s \in (\pi/2, 3\pi/2) \subset \mathbb{T}^1$ , and the other way around of points in  $\partial\Sigma_c^-$ , which are tangencies for  $X_2$ .

The points  $p = (x, y, s) \in \partial\Sigma_c^\pm$  with  $s = \pi/2 + k\pi$  with  $k \in \mathbb{Z}$  satisfy  $X_i^2 f(p) = 0$  and  $X_i^3 f(p) \neq 0$ , and therefore they are cubic tangencies. Generically, in 3-dimensional systems these points are isolated. In this system, they are the points

$$(-F + 1, 0, \pi/2), \quad (-F - 1, 0, 3\pi/2) \quad \text{for } X_1$$

and

$$(F + 1, 0, \pi/2), \quad (F - 1, 0, 3\pi/2) \quad \text{for } X_2.$$

In [Tei93] these points are called *cusps* and the trajectory through them is not only tangent to  $\Sigma$  but also to  $\partial\Sigma_c^\pm$ . In contrast the folds form curves in  $\Sigma$ .

**Remark 1.1.** *As it is already known and will be recalled in Section 1.3, the tangency points play an important role in the nonsmooth bifurcations of periodic orbits: a periodic orbit undergoes a sliding bifurcation precisely when it passes through one of these points.*

*The codimension of the bifurcation is also clear in this setting. Since the folds generically form curves in  $\Sigma$ , the fact that a periodic orbit crosses  $\Sigma$  through a fold is a codimension-1 phenomenon. Nevertheless, cusps are isolated points in  $\Sigma$ , so the periodic orbit will encounter these points as a codimension-2 phenomenon.*

**Remark 1.2.** *We observe that system (3) can be called dissipative since it has a sliding region which acts as an “attractor”. In [Kun00] the system  $\ddot{x} = -x + \text{sgn}(x) + p(t)$  with a periodic function  $p$  was also considered. For this conservative (Hamiltonian) nonsmooth dynamical system, the existence of periodic and bounded solutions was studied, using differential inclusion and KAM techniques, but the study of bifurcations was not carried out.*

### 1.3 Bifurcations of periodic orbits and symmetries in Filippov systems

As we explained in Section 1.1, besides the classical bifurcations, Filippov systems can undergo other types of bifurcations due to the discontinuity. One of the main sources of these new kind of bifurcations

(usually called *discontinuity induced bifurcations*), is the change of interaction between invariant objects and the sliding region. Focusing on bifurcations of periodic orbits, the planar case was studied in [KRG03].

For 3-dimensional Filippov systems the discontinuity induced bifurcations of periodic orbits are not yet completely understood and there are few results about their existence in concrete systems. The main work done in this area deals with bifurcations in which the periodic orbit persists and only changes its interaction with the sliding region. In [dBKN03], the authors study numerically this kind of interaction focusing on several models for dry-friction oscillators. Assuming that the periodic orbit is persistent, they study in great detail four cases which they call *grazing-sliding*, *switching-sliding*, *crossing-sliding* and *adding-sliding*, denoted as *gs*, *cs*, *ss* or *as* respectively. Bifurcations in which the periodic orbit is not persistent have been only numerically studied for systems in  $\mathbb{R}^3$  in [dBBCK08]. A recent study of bifurcations of periodic orbits from the point of view of Catastrophe Theory can be found in [JH].

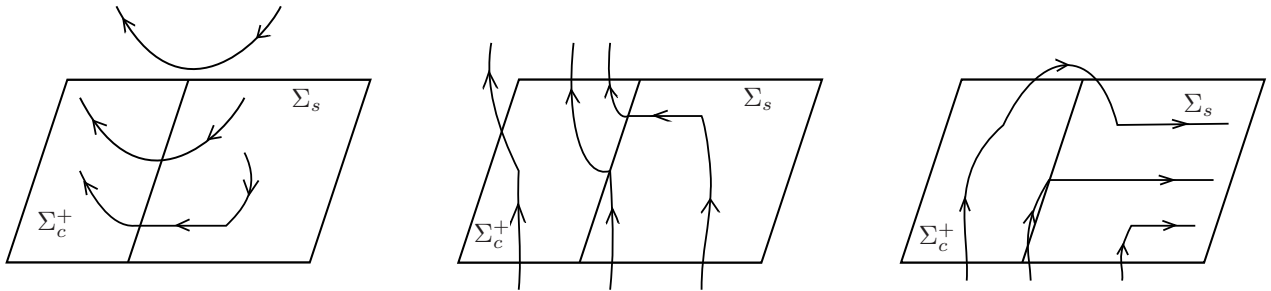


Figure 2: The *grazing-sliding*, *crossing-sliding* and *switching-sliding* bifurcations.

In this paper we will analyze examples of the first three cases (see Figure 2). For general systems, the *grazing-sliding* bifurcation occurs when the periodic orbit hits  $\Sigma$  at a point of  $\partial\Sigma_c^+$  ( $\partial\Sigma_c^-$ ) which is a visible tangency. Hence, for nearby parameter values, either the periodic orbit belongs to  $G_1$  or  $G_2$  and does not hit  $\Sigma$ , or the periodic orbit has a small piece of sliding motion.

The *crossing-sliding* bifurcation corresponds to a periodic orbit which crosses  $\Sigma_c^+$  ( $\Sigma_c^-$ ) and tends to  $\partial\Sigma_c^+$  ( $\partial\Sigma_c^-$ ) as the parameter tends to the bifurcation value. For different parameter values, as in the grazing-sliding bifurcation, a small segment of sliding motion appears in the periodic orbit.

Finally, the *switching-sliding* bifurcation corresponds to the case when the bifurcating periodic orbit has a piece of regular trajectory, for instance in  $G_2$ , then hits  $\Sigma$  in an invisible tangency in  $\partial\Sigma_c^+$  ( $\partial\Sigma_c^-$ ) and then slides. Thus, after the regular motion, there is a complete sliding motion, that is, both edges of it belong also to  $\partial\Sigma_c^\pm$ . Then, when the system is perturbed, on one side the periodic orbit does regular motion in  $G_2$  and then slides, and on the other side, does regular motion in  $G_2$ , then in  $G_1$  and finally slides.

The codimension-2 nonsmooth bifurcations of periodic orbits have been less well studied. As we said at the end of Section 1.2, all the previous bifurcations correspond to codimension-1 bifurcations, due to the fact that the folds form curves in  $\Sigma$ . But if we ask the periodic orbit to have a more degenerate tangency with  $\Sigma$ , as it is the case of a cusp, the phenomenon can only be encountered in two parameter families, that is, it is a codimension-2 bifurcation. In [KdBC<sup>+</sup>06, KdB05], the authors study numerically some codimension-2 bifurcations of periodic orbits and show that the presence of cusp points in the

periodic orbit is one of the main sources of codimension-2 bifurcations.

System (3), as happens in some of the examples of [KdBC<sup>+</sup>06, KdB05], has a symmetry, which is given by

$$R(x, y, s) = (-x, -y, s + \pi). \quad (7)$$

Thus, since system (3) has only one periodic orbit in the range of parameters we will study, we will look for a symmetric one. Otherwise would exist two different periodic orbits one being the symmetric of the other. Therefore, the piece of the periodic orbit for  $s \in (\pi, 2\pi)$ , will be symmetric with respect to its piece for  $s \in (0, \pi)$  and will undergo symmetric bifurcations. That is, the grazing-sliding, crossing-sliding and switching-sliding, and also the codimension-2 bifurcations, will come in pairs, one in each of both half periods.

## 1.4 Previous results for the dry-friction oscillator

The dry-friction oscillator has already been studied by several authors using different approaches, see for instance [CS06, CSS07, Kun00, KdBC<sup>+</sup>06, KdB05, dBKN03].

Using differential inclusion techniques, Kunze in [Kun00] (see page 40) established the existence of periodic orbits in system (3) when  $F > 0$ . His results are summarized in the following theorems.

**Theorem 1.3.** *Provided  $F \in (0, 1)$  and  $\omega \neq 1$ , system (3) has exactly one  $2\pi/\omega$ -periodic solution  $\Gamma_{\omega, F}(t) = (x^*(t), y^*(t), s^*(t))$  and it is asymptotically stable. That is, for any other solution  $(x(t), y(t), s(t))$  of system (3),*

$$(x(t) - x^*(t))^2 + (y(t) - y^*(t))^2 \longrightarrow 0 \text{ as } t \longrightarrow +\infty. \quad (8)$$

**Theorem 1.4.** *Provided  $F > 1$  and  $\omega \neq 1$ , there exists a family of periodic orbits  $\Gamma_{\omega, F}^c(t) = (c, 0, \omega t)$  for  $c \in [-F + 1, F - 1]$  of system (3). Moreover, if  $(x(t), y(t), s(t))$  is any other solution of (3), there exists  $c \in [-F + 1, F - 1]$  such that*

$$(x(t) - c)^2 + y(t)^2 \rightarrow 0 \text{ as } t \rightarrow +\infty. \quad (9)$$

**Remark 1.5.** *The case  $\omega = 1$  is the resonant case and it has unbounded motion, for certain range in  $F$ . We will not study this case, which has been considered in [Kun00] in great detail.*

The approach in [Kun00] does not give any information about the behaviour of the trajectories and their bifurcations and, for instance, one can not know whether the periodic orbit intersects the sliding region or not. Therefore, with these techniques, one is unable to detect sliding bifurcations and hence distinguish between stick and stick-slip motions.

For the case  $F > 1$ , the form of the periodic orbits  $\Gamma_{\omega, F}^c$  is known and they are contained in  $\Sigma_s$ . Improving on previous work (see [Fei94], [KdBC<sup>+</sup>06]), the behaviour of the periodic orbit was studied numerically in [KP08] for parameters in the range  $F \in (0, 1)$  and  $\omega^{-1} \in (1, 8)$ . Their bifurcation diagram is reproduced in Figure 3.

In [KP08], the authors compute the codimension-1 sliding bifurcation curves for the periodic orbit using numerical continuation techniques, and discover codimension-2 sliding bifurcation points. These codimension-1 curves correspond to the bifurcations explained in Section 1.3. The codimension-2 sliding bifurcation points are shown to act as organizing centers of the codimension-1 sliding bifurcations, and are then unfolded to explain dynamical features of the dry friction oscillator.

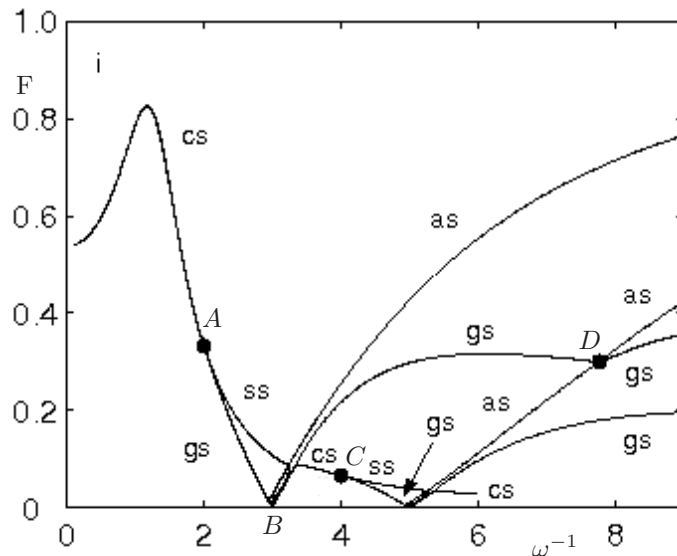


Figure 3: Bifurcation diagram in [KP08].

We will study analytically in Section 3 the system and detect infinitely many codimension-2 bifurcation points  $A_n := (\omega_n^{-1}, F_n) = (2n, 1/(4n^2 - 1))$  and we will compute analytically the periodic orbit in this case, using the fact that it crosses  $\Sigma$  (non-transversally) through the cusp point. We will then analyze rigorously the behaviour of the periodic orbit for parameters in a neighbourhood of these points, proving the existence of three codimension-1 bifurcation curves which emanate from them. We then focus our attention on point  $A_1$ , called  $A$  in [KP08], and give some asymptotic expansions of these curves that will be compared with numerical computations.

In Section 4 we will study the system when  $F$  is small, that is, considering the nonsmooth system as a small perturbation of an integrable smooth system. We will see that for  $\omega \neq 1/(2n + 1)$ , where  $n$  is an integer, the nonsmooth periodic orbit behaves as the corresponding smooth symmetric one for  $F = 0$ . For  $\omega = 1/(2n + 1)$  we also show that the points  $B_n := (\omega_n^{-1}, F_n) = (2n + 1, 0)$  are codimension-2 bifurcation points. The first of them  $B_1 := (\omega_1^{-1}, F_1) = (3, 0)$  was already numerically detected and carefully studied in [KP08]. In Section 5, we study analytically this first point  $B_1$  and examine the codimension-1 bifurcations around it. The study of  $B_n$ , for  $n > 1$ , seems more cumbersome. Even if for  $n > 1$  we can give some partial results in sectorial neighbourhoods  $S_1^\pm$  of the points  $B_n$ , the dynamics around these points can be more complex and needs more study.

We recall that, since for parameters  $F \in (0, 1)$  and  $\omega^{-1} \in (1, 8)$  the periodic orbit is unique, it has to be symmetric with respect to  $R$  in (7). For this reason, our approach will be to look for a symmetric periodic orbit and then we will have to describe only half of the period and our analysis will be considerably simplified.

## 2 Crossing periodic orbits

In this section we will obtain formulas for the one-turn crossing periodic orbit of system (3) and conditions for it to exist, which will be used to study the sliding bifurcations that that periodic orbit undergoes. We want to point out that we look for it assuming that it makes only one turn per period, that is, it only crosses  $\Sigma$  twice in every period. The periodic orbit of the system will satisfy this condition for a certain range of parameters. There are other values of the parameters for which the periodic orbit crosses  $\Sigma$  more than twice in every period, as it was seen numerically in [KP08]. Nevertheless, in this paper we restrict ourselves to study the one-turn crossing periodic orbit and its sliding bifurcations.

Consider the trajectory  $\Gamma_{\omega,F}(t) = (x(t), y(t), s(t))$  with initial condition  $(x_0, 0, s_0) \in \Sigma_c^+$ . Then, since the periodic orbit leaving this point (for certain  $s_0$ , yet to be determined) has to stay in  $G_1$  until it hits  $\Sigma$  again symmetrically after time  $\pi/\omega$ , the following equations have to hold:

$$\begin{cases} x(\pi/\omega) = -x_0 \\ y(\pi/\omega) = 0. \end{cases} \quad (10)$$

These equations can be explicitly solved to give the periodic orbit for certain range of the parameters as it can be seen in the following proposition. Of course not every solution of equations (10) gives a periodic orbit of system (3), since this solution can cross  $\Sigma$  for  $t \in (0, \pi/\omega)$  and therefore be a solution of  $X_1$  but not a solution of the Filippov system.

**Proposition 2.1.** *Equations (10) can be explicitly solved provided  $\omega \neq 1/(2n+1)$ ,  $n \in \mathbb{N}$ , and*

$$\left| F \frac{\omega^2 - 1}{\omega} \frac{\sin(\pi/\omega)}{1 + \cos(\pi/\omega)} \right| \leq 1. \quad (11)$$

to give the solution

$$\Gamma_{\omega,F}(t) = \begin{cases} x(t) = F \cos t + F \frac{\sin(\pi/\omega)}{1 + \cos(\pi/\omega)} \sin t - F + \frac{1}{1 - \omega^2} \sin(\omega t + s_0) \\ y(t) = -F \sin t + F \frac{\sin(\pi/\omega)}{1 + \cos(\pi/\omega)} \cos t + \frac{\omega}{1 - \omega^2} \cos(\omega t + s_0) \\ s(t) = s_0 + \omega t \end{cases} \quad (12)$$

for  $t \in (0, \pi/\omega)$ , where  $s_0$  is given by

$$s_0 = 2\pi - \arccos\left(F \frac{\omega^2 - 1}{\omega} \frac{\sin(\pi/\omega)}{1 + \cos(\pi/\omega)}\right). \quad (13)$$

For  $t \in (\pi/\omega, 2\pi/\omega)$ ,  $\Gamma_{\omega,F}(t)$  is given by the symmetry (7).

Moreover, this solution corresponds to a symmetric periodic orbit of system (3) which does not intersect  $\Sigma_s$  and crosses once  $\Sigma_c^+$  and  $\Sigma_c^-$  every period, provided the following conditions hold

$$x(0) - \sin s(0) \leq -F \quad (14)$$

$$y(t) > 0 \text{ for } t \in (0, \pi/\omega). \quad (15)$$

**Remark 2.2.** *We want to point out that for the parameters to which last proposition can not be applied, that is, for the parameters for which the periodic orbit given by (12) and (13) does not exist, the periodic*

orbit which does exist may not necessarily hit the sliding zone  $\Sigma_s$  (and therefore it may not perform stick-slip motions). In Proposition 2.1 we have looked for crossing periodic orbits making one turn per period, but for other range of the parameters where Proposition 2.1 fails, the periodic orbit can be also crossing but making more turns. In fact, in [KP08], it was seen numerically that in a sectorial neighbourhood of  $B_1 = (\omega^{-1}, F) = (3, 0)$  in the parameter space, the corresponding periodic orbit does not hit  $\Sigma_s$  and makes two turns per period. We conjecture that an analogous behaviour occurs around the points  $B_n = (\omega^{-1}, F) = (2n + 1, 0)$ .

**Remark 2.3.** Condition (14) can also be written as:

$$\frac{\omega^2}{1 - \omega^2} \sin s_0 \leq -F \quad (16)$$

and ensures, jointly with (10), that the crossing points  $(x(0), y(0), s(0))$  and  $(x(\pi/\omega), y(\pi/\omega), s(\pi/\omega))$  belong to  $\Sigma_+^c$  and  $\Sigma_-^c$  respectively.

Condition (16), using (13), gives a necessary condition in the parameter space for these orbits to exist, namely:

$$F \leq \frac{1}{\frac{1-\omega^2}{\omega^2} \sqrt{1 + \left( \frac{\omega \sin(\pi/\omega)}{1 + \cos(\pi/\omega)} \right)^2}} \quad (17)$$

Finally, condition (15) ensures that these points  $(x(0), y(0), s(0))$  and  $(x(\pi/\omega), y(\pi/\omega), s(\pi/\omega))$  are the only points of the periodic orbit that belong to  $\Sigma$ .

*Proof of Proposition 2.1.* Since  $X_1$  is a linear vector field, provided  $\omega \neq 1/(2n + 1)$ , one can easily obtain their solutions and impose equations (10) to obtain (12), which depends on  $\omega$ ,  $F$  and  $s_0$ , where  $s_0$  satisfies the equation

$$\cos s_0 = F \frac{\omega^2 - 1}{\omega} \frac{\sin(\pi/\omega)}{1 + \cos(\pi/\omega)}. \quad (18)$$

This equation has a solution provided (11) holds and thus this condition is necessary to ensure the existence of the periodic orbit. On the other hand, when this condition holds, equation (18) has two solutions in every period. Nevertheless, only one of them gives a periodic orbit of system (3). Indeed, if we denote these solutions  $s_0^{(1)}$  and  $s_0^{(2)}$ , then  $\sin s_0^{(1)} > 0$  and  $\sin s_0^{(2)} < 0$ , and thus since  $\omega < 1$ , inequality (16) only can hold for  $s_0^{(2)}$ . Therefore  $s_0$  is given by (13).  $\square$

### 3 Analytic study of Codimension-2 bifurcations $A_n$

Checking analytically that conditions (14) (or equivalently (16)) and (15) hold is, in general, difficult. Nevertheless, this computation is considerably easier in the particular case  $\omega = 1/2n$ .

For  $\omega = 1/2n$ , condition (17) (and then (14)) holds  $F \leq \frac{1}{4n^2 - 1}$ . In addition, it can be seen that the crossing periodic orbit for  $F$  satisfying (17), that is,  $F \leq \frac{1}{4n^2 - 1}$ , exists until it undergoes a sliding bifurcation as the periodic orbit hits the cusp point at  $F = F_n = 1/(4n^2 - 1)$ . This phenomenon was numerically studied in [KP08] at the points  $A_1 = (\omega_1, F_1) = (1/2, 1/3)$ , and  $A_2 = (\omega_2, F_2) = (1/4, 1/15)$ , which were called  $A$  and  $C$  there respectively.

In fact, for parameter values at the points  $A_n = (\omega_n, F_n) = (\frac{1}{2n}, \frac{1}{4n^2 - 1})$ , the next lemma shows that the same phenomena occur.

**Lemma 3.1.** *At  $A_n = (\omega_n, F_n) = (\frac{1}{2n}, \frac{1}{4n^2-1})$ , the periodic orbit given by (12) exists. Moreover, for the half period in which the  $4n\pi$ -periodic orbit stays in  $G_1$ , the periodic orbit is given by*

$$\Gamma_{\omega_n, F_n}(t) = \begin{cases} x_{\omega_n, F_n}(t) = \frac{1}{4n^2-1}(\cos t - 1) - \frac{4n^2}{4n^2-1} \cos\left(\frac{t}{2n}\right) \\ y_{\omega_n, F_n}(t) = -\frac{1}{4n^2-1} \sin t + \frac{2n}{4n^2-1} \sin\left(\frac{t}{2n}\right) \\ s_{\omega_n, F_n}(t) = \frac{t}{2n} + \frac{3\pi}{2}, \end{cases} \quad (19)$$

with  $t \in (0, 2n\pi)$ , and the other half is given by the symmetry (7). Moreover,  $\Gamma_{\omega_n, F_n}(0) = (-\frac{4n^2}{4n^2-1}, 0, \frac{3\pi}{2})$  and  $\Gamma_{\omega_n, F_n}(2n\pi) = (\frac{4n^2}{4n^2-1}, 0, 5\pi/2)$ , which correspond to the cusp points in the boundaries of the sliding surface (that is  $\partial\Sigma_c^+$  and  $\partial\Sigma_c^-$  respectively).

Consequently, the points  $A_n$  correspond to codimension-2 bifurcation points.

*Proof.* It is straightforward to see that taking  $(\omega, F) = (\omega_n, F_n)$  satisfies condition (11), that the periodic orbit (12) exists and is given by (19). Moreover, since for  $t = 0$  this periodic orbit passes through the cusp, condition (14) also holds. Therefore, it only remains to check the fulfillment of condition (15). For that purpose, it is enough to check that  $y(t) > 0$  in all the extrema of  $y(t)$ , where we have taken  $y(t) = y_{\omega_n, F_n}(t)$  to simplify the notation. Since,

$$\dot{y}(t) = \frac{1}{4n^2-1} \left( \cos\left(\frac{t}{2n}\right) - \cos t \right)$$

it is straightforward to see that  $\dot{y}(t) = 0$  has two families of solutions

$$\begin{aligned} t_+^k &= \frac{2n}{2n-1} 2k\pi \quad \text{for } k \in \mathbb{Z} \\ t_-^k &= \frac{2n}{2n+1} 2k\pi \quad \text{for } k \in \mathbb{Z} \end{aligned}$$

To check that  $y(t_{\pm}^k) > 0$ , we use that

$$y(t_{\pm}^k) = \frac{1}{2n \pm 1} \sin\left(\frac{t_{\pm}^k}{2n}\right).$$

Since we are only interested in  $t_{\pm}^k$  such that  $t_{\pm} \in (0, 2n\pi)$  (modulus  $4n\pi$ ), we have that  $y(t_{\pm}^k) > 0$ .  $\square$

### 3.1 Codimension-1 bifurcations curves emanating from $A_n$

In this section we will focus our attention on the study of the codimension-1 bifurcation curves that emanate from  $A_n$ . The study of all the points  $A_n$  is analogous, and we will see that around them one obtains exactly the same behaviour (see [KP08] for the numerical study of  $A_1$  and  $A_2$ , called there  $A$  and  $C$  respectively). In fact, geometrically, the behaviour of the periodic orbit at all the  $A_n$  is the same. It leaves the cusp point  $(-\frac{4n^2}{4n^2-1}, 0, \frac{3\pi}{2}) = (-F_n - 1, 0, \frac{3\pi}{2})$  through  $G_1$  until it reaches, at time  $t = 2\pi n = \pi/\omega_n$ , the symmetric point  $(\frac{4n^2}{4n^2-1}, 0, \frac{5\pi}{2}) = (F_n + 1, 0, \frac{5\pi}{2})$ .

For this reason, the codimension-1 bifurcations that the orbit undergoes when the parameters move from  $A_n$  will be the same.

We prove, as shown numerically in [KdBC<sup>+</sup>06] in the case of  $A_1$  and  $A_2$ , that three curves, which correspond to codimension-1 bifurcations, emanate from points  $A_n$  in such a way as to divide the neighbourhood of  $A_n$  into three regions. These curves correspond to *grazing-sliding*, *switching-sliding* and *crossing-sliding* bifurcations.

We provide expressions (21), (22), (23) for these curves, valid around the points  $A_n$ . Nevertheless, the local asymptotic expansions for these curves will be only computed in the case of  $A_1$ , mainly to compare with the previous numerical results in [KP08]. In particular, around  $A_1$ , we see that between the crossing-sliding and grazing-sliding curves, and between the grazing-sliding and switching-sliding curves, the contact is only  $\mathcal{C}^1$ , but between the crossing-sliding and switching-sliding curves, the contact is  $\mathcal{C}^3$ .

We denote by  $\gamma_1^n$ ,  $\gamma_2^n$  and  $\gamma_3^n$  the codimension-1 sliding bifurcation curves which emanate from  $A_n$  and by  $R_1^n$ ,  $R_2^n$  and  $R_3^n$  the regions in between these curves (see Figure 4).

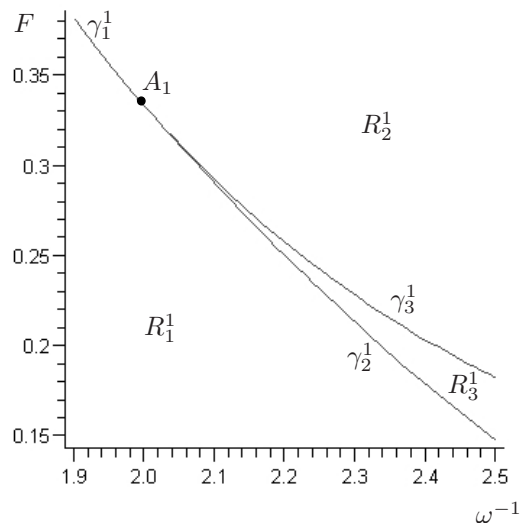


Figure 4: Bifurcation diagram near the point  $A_1$ .

Points in  $R_1^n$  correspond to the case of the periodic orbit  $\Gamma_{\omega,F}$  undergoing only *slip* motion, that is the orbit does not intersect the sliding region. Therefore it is just given by equation (12) and (13) and verifies (14) and (15). In  $R_2^n$ ,  $\Gamma_{\omega,F}$  undergoes *stick-slip* motion. In this region, taking as initial condition  $(x_0, 0, s_0) \in \partial\Sigma_c^+$ , the orbit goes through  $G_1$  until it hits again  $\Sigma_s$ , then slides until it reaches the boundary of the sliding region at the symmetric point  $(-x_0, 0, s_0 + \pi)$ . Finally, for parameters in  $R_3^n$ , after moving through  $G_1$ , the periodic orbit hits  $\Sigma_c^-$  instead of  $\Sigma_s$ , and then hits the sliding region from below and slides.

We shall now discuss these curves and regions in greater detail, and give expressions for the curves around  $A_n$ . Later, in Section 3.2, we will give local asymptotic expansion for these curves in the case of  $A_1$ .

The boundary of  $R_1^n$  is reached when one of conditions (14) and (15) no longer holds. In fact, depending on the value of  $\omega$ , the orbit can change in two different ways, giving rise to  $\gamma_1^n$  or  $\gamma_2^n$ . When  $\omega^{-1} < 2n$  and  $F$  is increased, condition (14) fails first, along  $\gamma_1^n$ . Here, the trajectory hits  $\Sigma$  in  $(x_0, 0, s_0) \in \partial\Sigma_c^+$ , in such a way that a further increase in  $F$  leads to the appearance of a small sliding trajectory. This is a *crossing-sliding* bifurcation. For  $\omega^{-1} > 2n$ , condition (15) fails first. Here another contact between the

trajectory and  $\Sigma$  appears in  $\partial\Sigma_c^+$  in every half period. Since this new contact is tangential,  $\gamma_2^n$  corresponds to a *grazing-sliding* bifurcation.

First, we focus our attention to the crossing-sliding curves  $\gamma_1^n$ . Given condition (11), condition (14) fails along  $\gamma_1^n$ , so that  $\Gamma_{\omega,F}(0) \in \partial\Sigma_c^+$ . Thus, in order to obtain an analytic expression for  $\gamma_1^n$ , it is enough to consider the condition

$$x(0) - \sin s(0) = -F \quad (20)$$

where  $(x(t), y(t), s(t))$  is the orbit defined in (12) and (13).

**Proposition 3.2.** *The curve  $\gamma_1^n$ , on which the crossing sliding bifurcation occurs, is given by*

$$F = \frac{1}{\frac{1-\omega^2}{\omega^2} \sqrt{1 + \left( \frac{\omega \sin(\pi/\omega)}{1+\cos(\pi/\omega)} \right)^2}}, \quad \omega^{-1} < 2n \quad (21)$$

close to the point  $A_n$  given in Lemma 3.1.

For parameters in this curve, the periodic orbit is given by (12), (13), and it holds that for  $t = 0$  and  $t = \pi/\omega$ , it belongs to  $\partial\Sigma_+^c$  and  $\partial\Sigma_-^c$  respectively.

*Proof.* Equation

$$x(0) - \sin s(0) = -F$$

where  $(x(t), y(t), s(t))$  is the orbit defined in (12) and (13), leads straightforwardly to (21). Moreover, it is clear that then (12) satisfies condition (14). Therefore, to assure that (12) corresponds to a periodic orbit of (3), it only remains to check that condition (15) also holds.

First we check the condition for  $t \in (0, \pi/\omega)$  close to  $t_+ = 0$  and  $t_- = \pi/\omega$ . Since for these points the periodic orbit passes through a fold in  $\Sigma$ , one has that  $y(t_{\pm}) = \dot{y}(t_{\pm}) = 0$ . To assure that close to these points  $y(t) > 0$ , it is enough to compute  $\ddot{y}(t_{\pm})$ , which is given by

$$\ddot{y}(t_{\pm}) = F(\pm\omega^2 - 1) \frac{\sin(\pi/\omega)}{1 + \cos(\pi/\omega)}$$

and therefore, since  $\omega^{-1} < 2$ , one has that  $\ddot{y}(t_{\pm}) > 0$ . Hence, there exists  $\delta > 0$  small enough such that  $y(t) > 0$  for  $t \in (0, \delta) \cup (\pi/\omega - \delta, \pi/\omega)$ . To check condition (15) for  $t \in [\delta, \pi/\omega - \delta]$ , it is enough to use that this set is compact and that  $y(t)$  is close to the  $y$  component of the periodic orbit for parameters in  $A_n$ , which is given by  $y_{\omega_n, F_n}(t)$  in (19). Thus, since  $y_{\omega_n, F_n}(t) > 0$  for  $t \in [\delta, \pi/\omega - \delta]$ , for  $\omega^{-1}$  close to  $2n$  this fact implies that  $y(t) > 0$  for  $t \in [\delta, \pi/\omega - \delta]$ .  $\square$

The form of the periodic orbit for values along curve  $\gamma_1^1$  can be seen in Figure 5.

The second curve which emanates from  $A_n$  is called  $\gamma_2^n$  and on it grazing-sliding bifurcations take place. If we consider the prolongation of the curve  $\gamma_1^n$  to  $\omega^{-1} > 2$ , it is easy to check, analogously to the proof of Proposition 3.2, that condition (15) does not hold. Therefore, for parameters below this curve must exist a curve  $\gamma_2^n$  where this condition fails first giving rise to the grazing-sliding bifurcation. In order to derive an expression for  $\gamma_2^n$  we do not use equations (12) and (13) anymore because the equation  $y(t) = 0$  can not be solved explicitly. Instead, we consider the equations which determine the behaviour of the periodic orbit at the grazing-sliding bifurcation.

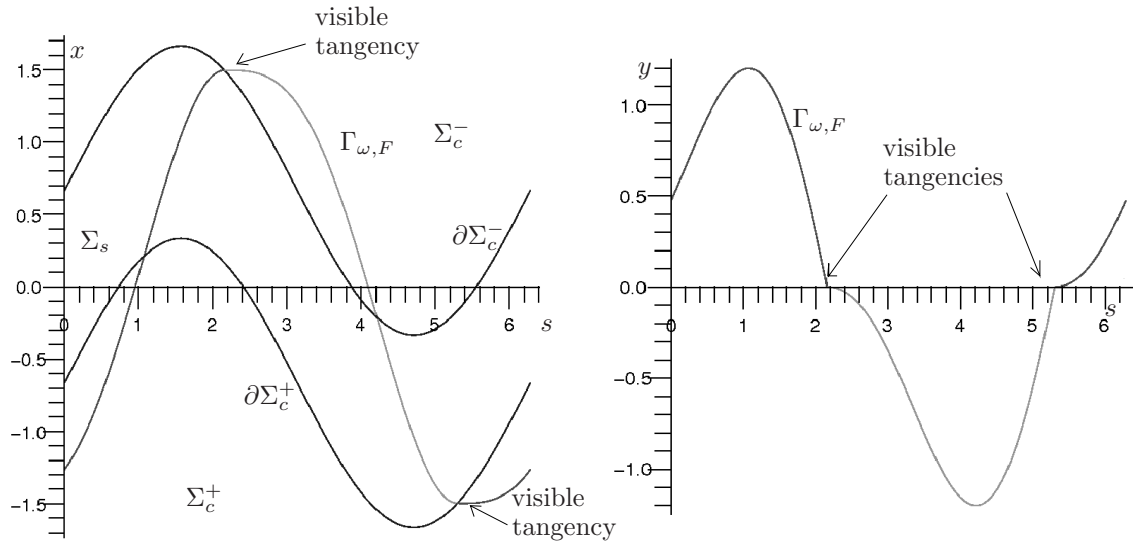


Figure 5: Projection of  $\Gamma_{\omega,F}$  onto the  $(s, x)$  and  $(s, y)$  planes respectively for parameters in the curve  $\gamma_1^1$ . The tangency points occur approximately at  $s = 2.2$  and  $s = 2.2 + \pi$ .

We look for this periodic orbit taking as initial condition a visible tangency point  $z_0 = (x_0, 0, s_0) \in \partial\Sigma_c^+$ , namely  $x_0 = -F + \sin(s_0)$  and  $s_0 \in (\pi/2, \pi) \cup (3\pi/2, 2\pi)$  (see Figure 6), whose trajectory can be obtained easily in terms of  $s_0$ . Thus, the corresponding trajectory  $\Gamma_{\omega,F}(t) = (x(t), y(t), s_0 + \omega t)$  hits  $\Sigma$  backwards and forwards in time at some symmetric points  $(x_1, 0, s_1) \in \Sigma_c^+$  and  $(-x_1, 0, s_1 + \pi) \in \Sigma_c^-$ , at times  $-h$  and  $\pi/\omega - h$  respectively for some  $h \in (0, \pi/\omega)$  along trajectories of  $X_1$ .

**Proposition 3.3.** *The curve  $\gamma_2^n$  is defined implicitly for suitable values  $h$  and  $s_0$  and for  $\omega^{-1} > 2$  by the equations*

$$\begin{cases} y(\pi/\omega - h) = 0 \\ y(-h) = 0 \\ x(\pi/\omega - h) + x(-h) = 0 \end{cases} \quad (22)$$

where  $(x(t), y(t), s(t))$  is the trajectory of  $X_1$  with initial condition at the fold  $z_0 = (x_0, 0, s_0) \in \partial\Sigma_c^+$  with  $x_0 = -F + \sin(s_0)$ .

*Proof.* It is straightforward to check that the fulfillment of equations (22) is a necessary condition to undergo a grazing-sliding bifurcation. On the other hand, for  $\omega_n^{-1} = 2n$ , the solution of (22) is given by  $F_n = 1/(4n^2 - 1)$ ,  $h = 0$  and  $s_0 = 3\pi/2$ , and the corresponding periodic orbit is (19). Nevertheless, the Implicit Function Theorem can not be applied directly since equations in (22) are degenerate close to  $A_n$  since the orbit passes through the cusp point. Therefore, one has to rescale the variables and the equations first. Taking  $\omega^{-1} = 2n + \varepsilon$  and considering the function

$$\mathcal{G}(F, h, s_0, \varepsilon) = (\varepsilon^{-1}y(\pi/\omega - h), \varepsilon^{-3}y(-h), \varepsilon^{-1}(x(\pi/\omega - h) + x(-h)))$$

with equations (22) rescaled and performing the change  $(F, h, s) = (F_n + \varepsilon\bar{F}, \varepsilon\bar{h}, 3\pi/2 + \varepsilon\bar{s})$ , the Implicit Function Theorem can be applied around the point  $(\bar{F}, \bar{h}, \bar{s}) = (-4/9, 3\pi/4, \pi/8)$ . This theorem gives us a

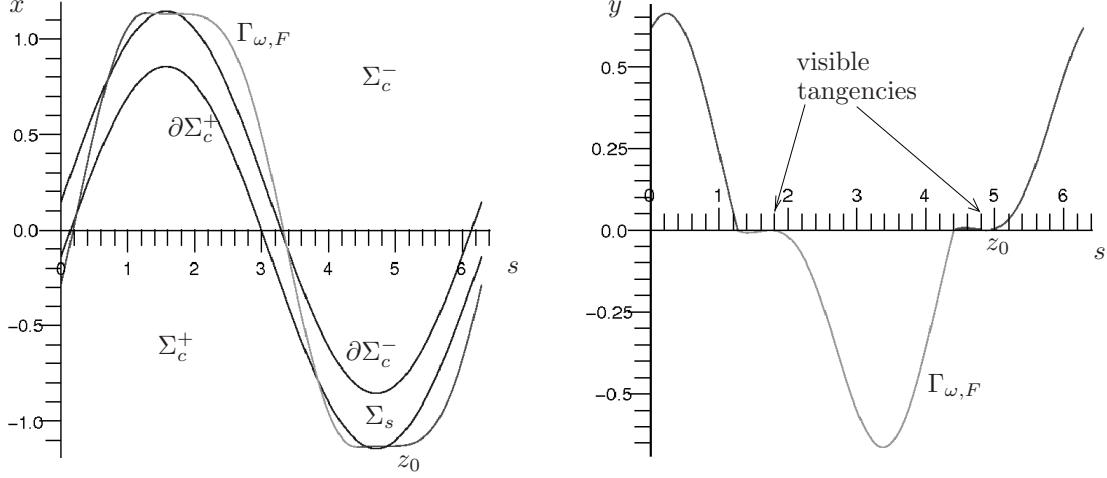


Figure 6: Projection of  $\Gamma_{\omega,F}$  onto the  $(s, x)$  and  $(s, y)$  planes respectively for parameters in the curve  $\gamma_2^1$ . The grazing points occurs approximately at  $s = s_0 = 4.9$  and  $s = s_0 - \pi$ .

curve  $F \equiv F(\omega)$  in a neighbourhood of  $\omega^{-1} = 2n$  in the parameter space, nevertheless it only corresponds to a bifurcation curve for  $\omega^{-1} > 2$ , since for  $\omega^{-1} < 2$ , as we saw in Proposition 3.2, condition (14) fails first.  $\square$

As it will be done in Section 3.2 for  $n = 1$ , using equation (22), one can obtain local expansions of the curves  $\gamma_2^n$  by expanding the variables  $F$ ,  $h$  and  $s_0$  in power series of  $\varepsilon = \omega^{-1} - 2n$ .

Once we have crossed  $\gamma_2^n$ , for  $(\omega^{-1}, F) \in R_3^n$ , in every half period, the periodic orbit visits both  $G_1$  and  $G_2$  once and then slides. Switching-sliding occurs on the boundary of this region (see Figure 7), in which the periodic orbit consists, in every half period, of a trajectory arriving to an invisible tangency followed by sliding, then a visible tangency and a regular trajectory.

We look for the periodic orbit  $\Gamma_{\omega,F}(t) = (x(t), y(t), s(t))$  as the trajectory with initial condition  $z_0 = (-F + \sin s_0, 0, s_0) \in \partial\Sigma_c^+$ ,  $s_0 \in (\pi, 2\pi)$  (see Figure 7). This orbit hits  $\Sigma$  again, in  $\partial\Sigma_c^-$ , after a piece of regular orbit in  $G_1$ , at a point  $(F + \sin s_1, 0, s_1) \in \partial\Sigma_c^-$  after time  $t_0 = (s_1 - s_0)/\omega$ . From this point the trajectory slides until  $(F + \sin s_1, 0, 5\pi - s_1) \in \partial\Sigma_c^-$ . As we want the periodic orbit to be symmetric, this last point has to satisfy

$$(F + \sin s_1, 0, 5\pi - s_1) = (F - \sin s_0, 0, s_0 + \pi),$$

which holds provided  $s_1 = 4\pi - s_0$ , and then  $t_0 = (4\pi - 2s_0)/\omega$ .

**Proposition 3.4.** *The curve  $\gamma_3^n$  is defined implicitly for suitable values of  $s_0$  and for  $\omega^{-1} > 2$  by the equations*

$$\begin{cases} x((4\pi - 2s_0)/\omega) = F - \sin(s_0) \\ y((4\pi - 2s_0)/\omega) = 0 \end{cases} \quad (23)$$

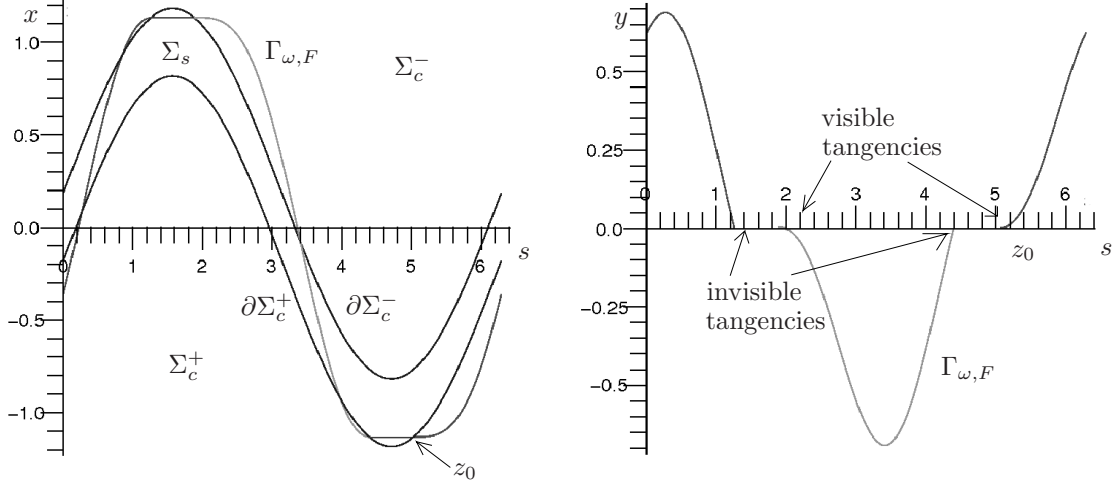


Figure 7: Projection of  $\Gamma_{\omega,F}$  onto the  $(s, x)$  and  $(s, y)$  planes respectively for parameters in curve  $\gamma_3^1$ . The visible tangencies are approximately at  $s = s_0 = 5$  and  $s = s_0 - \pi$  and the invisible ones at  $s = 4.4$  and  $s = 4.4 - \pi$ .

where  $(x(t), y(t), s(t))$  is the trajectory of  $X_1$  leaving from the fold  $z_0 = (x_0, 0, s_0) \in \partial\Sigma_c^+$  with  $x_0 = -F + \sin(s_0)$ .

*Proof.* It is straightforward to check that the fulfillment of equation (23) is a necessary condition to undergo a switching-sliding bifurcation. On the other hand, at the point  $A_n = (\omega_n^{-1}, F_n) = (2n, 1/(4n^2 - 1))$ , the solution of (23) is given by  $s_0 = 3\pi/2$ , and the corresponding periodic orbit is (19).

To prove that (23) defines implicitly the curve, it is enough to use the Implicit Function Theorem, which in this case can be applied directly with no need of rescaling. Thus, we obtain a curve  $F \equiv F(\omega)$  in a neighbourhood of  $\omega^{-1} = 2$ . Nevertheless, as in Proposition 3.3, this curve only corresponds to a bifurcation curve for  $\omega^{-1} > 2$ .

□

### 3.2 Local expansions of $\gamma_1^1$ , $\gamma_2^1$ and $\gamma_3^1$

In this section we provide some local expansions in terms of  $\varepsilon = \omega^{-1} - 2$  of the codimension-1 bifurcations curves  $\gamma_1^1$ ,  $\gamma_2^1$  and  $\gamma_3^1$ , which emanate from point  $A_1$  and which have been studied in Propositions 3.2, 3.3 and 3.4.

**Proposition 3.5.** *The curves  $\gamma_1^1$ ,  $\gamma_2^1$  and  $\gamma_3^1$  are given, locally by  $F = \gamma_i(\varepsilon)$  where  $\varepsilon = \omega^{-1} - 2$  as*

$$\gamma_1^1(\varepsilon) = \frac{1}{3} - \frac{4}{9}\varepsilon + \left(\frac{13}{27} - \frac{\pi^2}{96}\right)\varepsilon^2 + \frac{1}{6}\left(\frac{7}{48}\pi^2 - \frac{80}{27}\right)\varepsilon^3 + \left(\frac{121}{243} - \frac{127}{3456}\pi^2 - \frac{23}{18432}\pi^4\right)\varepsilon^4 + \mathcal{O}_5(\varepsilon) \quad (24)$$

for  $\varepsilon < 0$ , and

$$\gamma_2^1(\varepsilon) = \frac{1}{3} - \frac{4}{9}\varepsilon + \left(\frac{13}{27} - \frac{13}{384}\pi^2\right)\varepsilon^2 + \mathcal{O}_3(\varepsilon). \quad (25)$$

$$\gamma_3^1(\varepsilon) = \frac{1}{3} - \frac{4}{9}\varepsilon + \left(\frac{13}{27} - \frac{\pi^2}{96}\right)\varepsilon^2 + \frac{1}{6}\left(\frac{7}{48}\pi^2 - \frac{80}{27}\right)\varepsilon^3 + \left(\frac{121}{243} - \frac{127}{3456}\pi^2 + \frac{1}{18432}\pi^4\right)\varepsilon^4 + \mathcal{O}_5(\varepsilon), \quad (26)$$

for  $\varepsilon > 0$ .

Therefore, the contact between  $\gamma_1^1$  and  $\gamma_2^1$  is  $\mathcal{C}^1$  while the contact between  $\gamma_3^1$  and  $\gamma_1^1$  is  $\mathcal{C}^3$  and between  $\gamma_3^1$  and  $\gamma_2^1$  is  $\mathcal{C}^1$ .

*Proof.* For  $\gamma_1^1$  we just need to use the explicit expression (21), and Taylor expand it at point  $A_1$  obtaining the desired result.

In the case of  $\gamma_2^1$ , we can solve equation (22) expanding the variables  $F$ ,  $h$  and  $s_0$  in power series of  $\varepsilon = \omega^{-1} - 2$  to obtain

$$\begin{cases} F = \frac{1}{3} + F_1\varepsilon + F_2\varepsilon^2 + \mathcal{O}_3(\varepsilon) \\ h = h_1\varepsilon + h_2\varepsilon^2 + \mathcal{O}_3(\varepsilon) \\ s_0 = \frac{3\pi}{2} + s_{0,1}\varepsilon + s_{0,2}\varepsilon^2 + \mathcal{O}_3(\varepsilon) \end{cases}$$

where the coefficients can be determined by straightforward computations giving the local expansion.

In the case of  $\gamma_3^1$ , we just need to solve (23) expanding  $(F, s_0)$  as

$$\begin{cases} F = \frac{1}{3} + \sum_{k=1}^4 F_k\varepsilon^k + \mathcal{O}_5(\varepsilon) \\ s_0 = \frac{3\pi}{2} + \sum_{k=1}^4 s_{0,k}\varepsilon^k + \mathcal{O}_5(\varepsilon) \end{cases}$$

where the coefficients can be determined by straightforward computations.

Comparing expressions (24), (25) and (26), one can see that the contact between  $\gamma_1^1$  and  $\gamma_2^1$  is only  $\mathcal{C}^1$  and the contact between  $\gamma_3^1$  and  $\gamma_1^1$  is  $\mathcal{C}^3$  and between  $\gamma_3^1$  and  $\gamma_2^1$  is  $\mathcal{C}^1$ .  $\square$

### 3.3 Comparison with previous numerical work

In Proposition 3.5 we have obtained local expansions for the codimension-1 bifurcation curves which emanate from point  $A_1$ . Now, we compare our analytical results with the numerical ones which were obtained in [KP08]. In Figure 8 we plot the two sets of the three curves and one can see that they fit very well close to point  $A_1$ .

## 4 The periodic orbit for $F$ small

In this section, we study system (3) for arbitrarily small  $F$ . For  $F = 0$ , system (3) becomes smooth and integrable, and it is straightforward to check that

1. For  $\omega \in \mathbb{R} \setminus \mathbb{Q}$ , there is a unique  $2\pi/\omega$ -periodic orbit  $\Gamma_{\omega,0}$ , which is symmetric with respect to (7). All other trajectories are quasiperiodic and rotate around the periodic orbit, densely filling invariant tori.

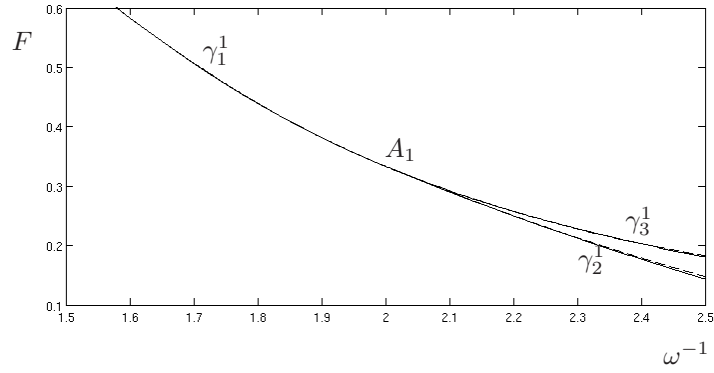


Figure 8: Comparison between the codimension-1 bifurcation curves emanating from point  $A_1$  obtained numerically in [KP08] (continuous line) and the local expansions obtained in this article (dashed line).

2. For  $\omega \in \mathbb{Q} \setminus \{1/n : n \in \mathbb{N}\}$ , there is a unique  $2\pi/\omega$ -periodic orbit  $\Gamma_{\omega,0}$  which is symmetric. All other trajectories are periodic with higher period and also rotate around the periodic orbit.
3. For  $\omega = 1/n$  for  $n \in \mathbb{N}$  (but  $\omega \neq 1$ ), all the trajectories are  $2\pi/\omega$ -periodic. Moreover, for even  $n$  among these periodic orbits there exist only one which is symmetric whereas for odd  $n$  all the periodic orbits are symmetric.

We want to study the behaviour of the  $2\pi/\omega$ -periodic orbit for the perturbed case  $F > 0$ , when the sliding region  $\Sigma_s$  is small. We recall that we already know the existence and uniqueness of the  $2\pi/\omega$ -periodic orbit for  $\omega \in (0, 1)$  and  $F \in (0, 1)$  from Theorem 1.3, which moreover is symmetric with respect to (7). As we will see in the next proposition, in most of the cases the nonsmooth periodic orbit is just the continuation of the unique symmetric smooth periodic orbit existing in the limiting case  $F = 0$ .

**Proposition 4.1.** *Let us consider system (3) with  $\omega^* \in (0, 1)$  but  $\omega^* \neq 1/(2n + 1)$ ,  $n \in \mathbb{N}$ . Then for  $(\omega, F)$  close enough to  $(\omega^*, 0)$ , there exists a unique  $2\pi/\omega$ -periodic orbit  $\Gamma_{\omega,F}$  which is symmetric with respect to (7) and does not hit the sliding surface. Moreover, in every half period, the orbit hits the discontinuity surface  $\Sigma$  only once in  $\Sigma_c^\pm$  and, in the half period for which it belongs to  $G_1$ , is given by (12) and (13).*

*Furthermore, if  $\Gamma_{\omega^*,0}$  is the unique symmetric periodic orbit given by (12) and (13) with  $F = 0$ ,  $\Gamma_{\omega,F} \longrightarrow \Gamma_{\omega^*,0}$  as  $(\omega, F) \rightarrow (\omega^*, 0)$ .*

*Proof.* The existence and uniqueness of the periodic orbit for  $F > 0$  is already known due to Theorem 1.3. We first prove that the periodic orbit is given by (12) and (13).

For  $\omega$  close enough to  $\omega^*$ , one has that  $\omega \neq 1/(2n + 1)$ ,  $n \in \mathbb{N}$ . On the other hand, taking  $F < F_0$  for certain  $F_0 \equiv F_0(\omega) > 0$ , condition (11) also holds. Therefore, (12) and (13) hold. Therefore, it only remains to check that conditions (14) and (15) hold, to ensure that (12) and (13) give a periodic orbit of (3).

Reducing  $F$  if necessary, one has that condition (17) holds, and this condition implies (14). We check (15) in two steps, first for  $t \in (0, \pi/\omega)$  close to  $t_+ = 0$  and  $t_- = \pi/\omega$ . Since for these points the

periodic orbit intersects  $\Sigma$ , one has  $y(t_{\pm}) = 0$ . To assure that close to these points,  $y(t) > 0$  it is enough to consider

$$\dot{y}(t_{\pm}) = \mp \left( F + \frac{\omega^2}{1 - \omega^2} \sin s_0 \right)$$

Therefore, using (16), which is equivalent to (14), already shown to hold, one obtains that  $\dot{y}(0) > 0$  and  $\dot{y}(\pi/\omega) < 0$  and therefore there exists  $\delta > 0$  small enough such that  $y(t) > 0$  for  $t \in (0, \delta) \cup (\pi/\omega - \delta, \pi/\omega)$ . For  $t \in [\delta, \pi/\omega - \delta]$ , we use that  $y(t)$  is close to the  $y$  component of  $\Gamma_{\omega^*, 0}$  (see (12)) which is given by

$$y_{\omega^*, 0}(t) = -\frac{\omega^*}{1 - (\omega^*)^2} \sin(\omega t)$$

Thus, since  $y_{\omega^*, 0}(t) > 0$  for  $t \in [\delta, \pi/\omega - \delta]$ , which is a compact set, taking  $(\omega, F)$  closer to  $(\omega^*, 0)$ , we have that  $y(t) > 0$ .

Once we know that the periodic orbit is given by (12) and (13), taking  $(\omega, F) \rightarrow (\omega^*, 0)$  in expression (12), it is straightforward to obtain the last statement.  $\square$

**Remark 4.2.** *The case  $\omega = 1/2n$ ,  $n \in \mathbb{N}$  with arbitrarily small  $F > 0$ , has the same behaviour as the case  $\omega \neq 1/n$ . That is, among the infinity of orbits existing in the smooth case  $F = 0$ , only the symmetric one does not break down, persisting for every value of the parameters in a neighbourhood of  $F = 0$  and  $\omega = 1/2n$ .*

#### 4.1 The codimension-2 bifurcation points $B_n$

Following Proposition 4.1, we know the behaviour of the periodic orbit for any  $(\omega, F)$  close enough to  $(\omega^*, 0)$  with  $\omega^* \neq 1/(2n + 1)$ . Moreover, close to the points  $B_n = (\omega_n^{-1}, F_n) = (2n + 1, 0)$ , there exist sectorial neighbourhoods  $S_1^{\pm}$  where the crossing symmetric periodic orbit given by Proposition 2.1 exists, and they correspond to the parameters for which conditions (14) and (15) hold. As it has been pointed out in Section 3, in general it is difficult to check when these conditions hold. Nevertheless, for the points  $B_n$  we already know, thanks to Proposition 4.1, that the sectorial neighbourhoods  $S_1^{\pm}$  exist.

In next proposition, whose proof is straightforward, we will see that, depending upon the path in these sectorial neighbourhoods  $S_1^{\pm}$  in parameter space we choose to approach the bifurcation point  $B_n$ , the limiting periodic orbit is different.

**Proposition 4.3.** *Let us consider parameters  $(\omega^{-1}, F) \in S_1^{\pm}$  in lines of the form*

$$\begin{cases} \omega^{-1} = 2n + 1 + k\delta \\ F = \delta \end{cases} \quad (27)$$

for  $\delta > 0$  small. Then, taking  $\delta \rightarrow 0$ , the crossing periodic orbit  $\Gamma_{\omega, F}$  given in Proposition 2.1 tends to the smooth periodic orbit

$$\Gamma_{1/(2n+1), 0}^k(t) = \begin{cases} x(t) = -\frac{2}{k\pi} \sin t + \frac{2(2n+1)}{k\pi} \sin\left(\frac{t}{2n+1}\right) - \frac{2n+1}{4\pi} \sqrt{\pi^2 \left(\frac{2n+1}{n^2+n}\right)^2 - \frac{64}{k^2}} \cos\left(\frac{t}{2n+1}\right) \\ y(t) = -\frac{2}{k\pi} \cos t + \frac{2}{k\pi} \cos\left(\frac{t}{2n+1}\right) + \frac{2n+1}{4\pi} \sqrt{\pi^2 \left(\frac{2n+1}{n^2+n}\right)^2 - \frac{64}{k^2}} \sin\left(\frac{t}{2n+1}\right) \\ s(t) = \frac{t}{2n+1} + s_0 \end{cases} \quad (28)$$

where  $s_0 = \frac{3}{2}\pi + \arcsin\left(\frac{8n(n+1)}{k\pi(2n+1)}\right)$ .

## 5 Analytic study of the codimension-2 bifurcation point $B_1$

The first case when Proposition 2.1 can not be applied is the point  $B_1 := (\omega^{-1}, F) = (3, 0)$ , whose study is the subject of this section. Throughout this section, for simplicity, we refer to  $B_1$  as  $B$ . The study of the other points  $B_n$  seems to be more involved and, as far as the authors know, these points have not been studied even numerically. At point  $B$ , the phase space is foliated by  $6\pi$ -periodic orbits, which are symmetric. The fact that the limiting periodic orbit depends upon the path in the parameter space considered to approach  $B$ , as it has been seen in Proposition 4.3, will lead to several bifurcations. In [KP08], six codimension-1 bifurcation curves which emanated from  $B$  were detected numerically. In this section, we will prove the existence of these curves and we will compute their local expansions. At the same time, we will show the behaviour of the periodic orbit for parameters belonging to these curves.

We denote these curves by  $\sigma_i^\pm$  for  $i = 1, 2, 3$  and the regions in between the curves are denoted by  $S_i^\pm$  for  $i = 1, \dots, 3$  and  $S_4$  (see Figure 9). In fact,  $S_1^- = R_1^1$ ,  $S_2^- = R_3^1$  and also  $\sigma_1^- = \gamma_2^1$ , which were studied in Section 3. Thus, in  $S_1^-$  the periodic orbit does not hit the sliding region and along  $\sigma_1^-$  undergoes a grazing-sliding bifurcation. In  $S_2^-$  it visits both  $G_1$  and  $G_2$  and then slides.

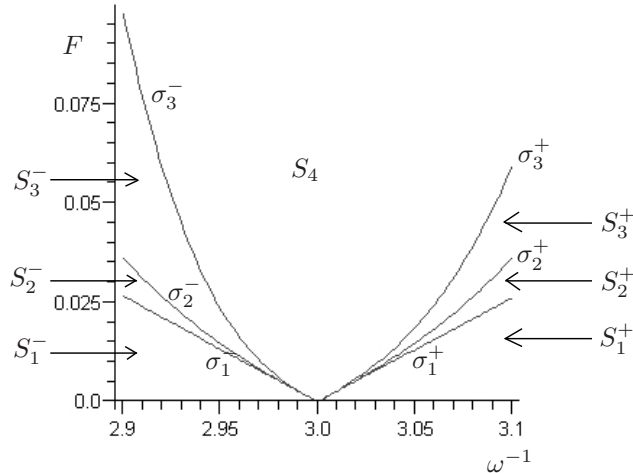


Figure 9: Codimension-1 bifurcations curves in a neighbourhood of point B

The curve  $\sigma_2^-$  corresponds to a switching-sliding bifurcation. Along it the periodic orbit consists, in every half period, of a trajectory arriving at an invisible tangency in  $\partial\Sigma_c^-$  followed by sliding, then a visible tangency in  $\partial\Sigma_c^+$  and a regular trajectory which visits both  $G_1$  and  $G_2$ . For parameters in  $S_3^-$ , the periodic orbit visits  $G_2$ ,  $G_1$  and  $G_2$  before it slides, and then leaves  $\Sigma$  through  $\partial\Sigma_c^+$  and has another segment of regular trajectory in  $G_1$ . The limiting behaviour corresponds to a crossing-sliding bifurcation

which occurs along  $\sigma_3^-$ . In this case, the periodic orbit has regular trajectories in  $G_2$ ,  $G_1$  and  $G_2$  and then hits  $\Sigma$  in  $\partial\Sigma_c^+$ . In region  $S_4$  the periodic orbit does not hit  $\Sigma_s$  and in every half period it crosses  $\Sigma$  three times always in  $\Sigma_c^\pm$ . The behaviour in the other regions and curves is symmetric. That is,  $\sigma_3^+$ ,  $\sigma_2^+$  and  $\sigma_1^+$  correspond to crossing-sliding, switching-sliding and grazing-sliding bifurcations respectively. For a more detailed explanation of the different behaviours, see [KP08].

## 5.1 Crossing periodic orbit in regions $S_1^\pm$

We begin the study of the neighbourhood of point  $B$  by analyzing regions  $S_1^\pm$  around it. As we showed in Section 3, the nonsmooth periodic orbit in regions  $S_1^\pm$  is given by (12) and (13) subject to conditions (11), (14) and (15).

As was seen in Proposition 3.3, the boundary of region  $S_1^-$  is reached when condition (15) fails, and the orbit undergoes a grazing-sliding bifurcation.

As we are using perturbation techniques, to look for a local expression of curve  $\sigma_1^-$  we need a good approximation of the periodic orbit. In the case of point  $A_n$ , the periodic orbit was well approximated by  $\Gamma_{\omega_n, F_n}$  in (19) which was the periodic orbit existing at the codimension-2 bifurcation point. Nevertheless, Proposition 4.1 fails in point  $B$  so that we do not know the first order approximation of  $\Gamma_{\omega, F}$  in this case. In the following lemma, whose proof is straightforward, we obtain the limiting periodic orbit and the slope of the curve  $\sigma_1^-$ .

**Lemma 5.1.** *The limiting smooth symmetric periodic orbit (28) obtained in Proposition 4.3, taking parameters (27) with  $\delta \rightarrow 0$ , is a one-turn crossing periodic orbit, that is crosses  $\Sigma$  only twice per period and transversally, provided  $|k| \leq 16\sqrt{5}/3\pi$ .*

Therefore,

$$m^\pm = \frac{1}{k^\pm} = \pm \frac{3\pi}{16\sqrt{5}}$$

are the slopes of the curves  $\sigma_1^\pm$ , and the limiting periodic orbit for parameters in these curves is just (28) with  $n = 1$  and  $k = k^\pm$ . Moreover, this periodic orbit intersects  $\Sigma$  tangentially at  $(\sin(s_0^\pm), 0, s_0^\pm)$  with

$$s_0^- = \frac{7\pi}{4} - \arcsin \frac{1}{\sqrt{5}} \quad \text{and} \quad s_0^+ = \frac{5\pi}{4} + \arcsin \frac{1}{\sqrt{5}}$$

respectively, and also in the corresponding symmetric points.

**Remark 5.2.** *The generalization of this result to the other points  $B_n$  seems more involved. Firstly, the proof of this lemma relies on finding double zeros of  $y(t)$  in (28). At  $B_1$ , this problem can be reduced to a degree two polynomial. Nevertheless, for  $n > 1$ , one obtains higher degree polynomials and then it is more difficult to obtain the tangency points analytically.*

*On the other hand, for  $n > 1$  the symmetric periodic orbits for  $F = 0$  can make more turns per period and then they can present more tangencies, and thus around points  $B_n$  it is expected that more bifurcations can occur. It would be interesting to study numerically the points  $B_n$  for  $n > 1$  to see which part of the structure encountered in  $B_1$  persists and which new bifurcations appear.*

In the forthcoming sections, we will see that these tangencies of the limiting periodic orbits make possible all the sliding bifurcations of the non-smooth periodic orbit undergone in the bifurcation curves

$\sigma_1^\pm - \sigma_3^\pm$ . Indeed, we will see that  $m^\pm$  are the slopes of all the bifurcation curves, and that the limiting orbit through these curves is given by (28) for  $k = k^\pm$  in all the cases.

## 5.2 The grazing-sliding bifurcation curves $\sigma_1^\pm$

Since  $\sigma_1$  is the curve  $\gamma_2^1$  which has been studied in Proposition 3.3, it has to satisfy the implicit equations (22).

**Proposition 5.3.** *The grazing-sliding codimension-1 bifurcation curve  $\sigma_1^-$  emanating from  $B$  is defined implicitly for suitable values  $h$  and  $s_0$  and for  $\omega^{-1} < 3$  close to  $\omega^{-1} = 3$  by the equations (22) given in Proposition 3.3.*

*Proof.* When  $(\omega^{-1}, F) \in \sigma_1^-$ , the parameters are given, up to first order, by (27) with  $k = k^-$ , so that the periodic orbit  $\Gamma_{\omega, F}$  is well approximated by (28) with  $n = 1$  and  $k = k^-$  which satisfies equations (22) when

$$h = \frac{3\pi}{4} \quad \text{and} \quad s_0 = \frac{7\pi}{4} - \arcsin \frac{1}{\sqrt{5}}.$$

Therefore, using the suitable rescaling and change of variables, applying the Implicit Function Theorem as we did in Proposition 3.3, it is straightforward to prove that equations (22) define implicitly  $\sigma_1^-$  for  $\omega^{-1}$  close enough to  $\omega^{-1} = 3$ . Nevertheless, it only corresponds to a bifurcation curve for  $\omega^{-1} < 3$ , since  $\omega^{-1} > 3$  implies  $F < 0$  which does not have physical meaning.  $\square$

Expanding the variables of equation (22) in power series of  $\varepsilon = \omega^{-1} - 3$  for  $\varepsilon < 0$  as

$$\begin{cases} F = -\frac{3}{80}\pi\sqrt{5}\varepsilon + F_2\varepsilon^2 + F_3\varepsilon^3 + \mathcal{O}_4(\varepsilon) \\ h = \frac{3\pi}{4} + h_1\varepsilon + h_2\varepsilon^2 + h_3\varepsilon^3 + \mathcal{O}_4(\varepsilon) \\ s_0 = \frac{7\pi}{4} - \arcsin \frac{1}{\sqrt{5}} + s_{0,1}\varepsilon + s_{0,2}\varepsilon^2 + s_{0,3}\varepsilon^3 + \mathcal{O}_4(\varepsilon), \end{cases}$$

one can obtain the local expansion of  $\sigma_1^-$ .

**Corollary 5.4.** *The local expansion of curve  $\sigma_1^-$  is given by*

$$\sigma_1^-(\varepsilon) = -\frac{3\pi\sqrt{5}}{80}\varepsilon - \frac{\sqrt{5}\pi}{1600}(-25 + 6\pi)\varepsilon^2 - \frac{1}{32000}\pi\sqrt{5}\left(195 - 110\pi + \frac{71}{2}\pi^2\right)\varepsilon^3 + \mathcal{O}(\varepsilon^4). \quad (29)$$

for  $\varepsilon < 0$ .

The proof of the existence and the computation of the local expansion for  $\sigma_1^+$  can be done analogously. Recall that in that case, the visible tangency with  $s_0 \in (\pi, 2\pi)$  belongs to  $\partial\Sigma_c^-$ . Therefore, one has to consider equations (22) around  $h = 9\pi/4$  and  $s_0 = 5\pi/4 + \arcsin(1/\sqrt{5})$ .

**Corollary 5.5.** *The local expansion of curve  $\sigma_1^+$  is given by*

$$\sigma_1^+(\varepsilon) = \frac{3\pi\sqrt{5}}{80}\varepsilon + \frac{\sqrt{5}\pi}{1600}(-25 + 6\pi)\varepsilon^2 + \frac{1}{32000}\pi\sqrt{5}\left(195 - 110\pi + \frac{71}{2}\pi^2\right)\varepsilon^3 + \mathcal{O}(\varepsilon^4), \quad (30)$$

for  $\varepsilon > 0$ .

### 5.3 The switching-sliding bifurcation curves $\sigma_2^\pm$

Once we have crossed  $\sigma_1^-$ , for  $(\omega^{-1}, F) \in S_2$ , in every half period, the periodic orbit visits both  $G_1$  and  $G_2$  once and then slides. Switching-sliding occurs on the boundary of this region (see Figure 10) in which the periodic orbit consist of regular trajectories in  $G_2$  and  $G_1$  arriving to an invisible tangency followed by sliding, then a visible tangency and a regular trajectory. The main difference between the curve  $\sigma_2^-$  and the curve  $\gamma_3$ , explained in Proposition 3.4, is that now the invisible tangency, where the regular orbit arrives in  $\Sigma$ , belongs to  $\partial\Sigma_c^-$  instead of  $\partial\Sigma_c^+$  (since  $F$  is very small).

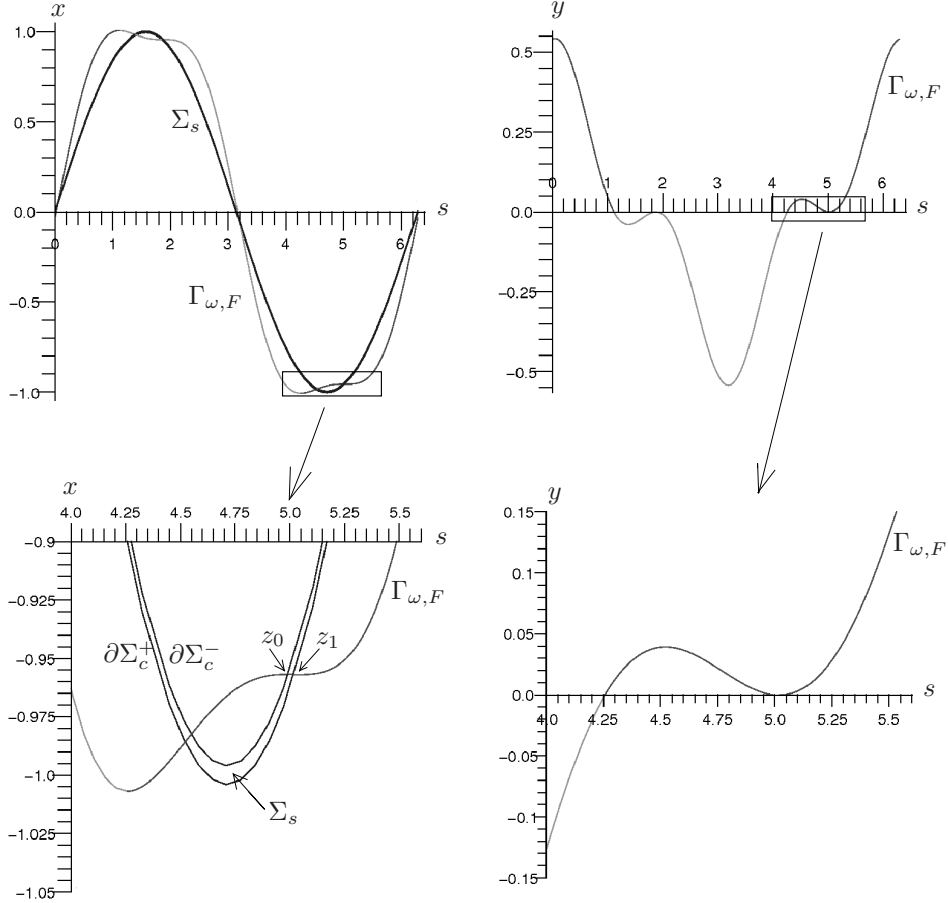


Figure 10: Projection of  $\Gamma_{\omega,F}$  onto the planes  $(s, x)$  and  $(s, y)$  respectively for parameters in the curve  $\sigma_2^-$  are given in the upper pictures. A zoom of the rectangle around the sliding motion is given in the lower pictures. In the left one, one can see  $z_0$  and  $z_1$  which are the limiting points of the sliding motion.

The construction of the periodic orbit is done as follows. We denote by  $z_0 = (F + \sin s_0, 0, s_0) \in \partial\Sigma_c^-$  and  $z_1 = (-F + \sin s_1, 0, s_1) \in \partial\Sigma_c^+$  the endpoints of the sliding motion (see Figure 10). Then we denote  $(x^0(t), y^0(t), s^0(t))$  as the trajectory leaving the first of these points in backward time and  $(x^1(t), y^1(t), s^1(t))$  as the trajectory leaving the second of these points in forward time.

Since the union of these trajectories has to occur in a half period and the two endpoints of this union

of trajectories have to be symmetric and to belong to  $\Sigma$ , the equations that have to hold on  $\sigma_2^-$  are

$$\begin{cases} F + \sin s_0 = -F + \sin s_1 \\ y^1(h) = 0 \\ y^0(h + (s_1 - s_0)/\omega - \pi/\omega) = 0 \\ x^1(h) + x^0(h + (s_1 - s_0)/\omega - \pi/\omega) = 0 \end{cases} \quad (31)$$

where we have used the fact that the time taken by the sliding motion is  $(s_1 - s_0)/\omega$ . The first equation denotes that in the sliding trajectories the  $x$  coordinate remains constant and the other ones that the two limiting points of this half periodic orbit belong to  $\Sigma$  and are symmetric.

**Proposition 5.6.** *The switching-sliding codimension-1 bifurcation curve  $\sigma_2^-$  emanating from  $B$  is defined implicitly for suitable values  $h$ ,  $s_0$  and  $s_1$ , and for  $\omega^{-1} < 3$  close to  $\omega^{-1} = 3$  by equations (31).*

*Proof.* Taking into account that the three bifurcations undergone along  $\sigma_1^-$ ,  $\sigma_2^-$  and  $\sigma_3^-$  involve sliding motion, and that the sliding region reduces to the curve  $x = \sin s$  when  $F$  tends to 0, one can easily see that the limiting periodic orbit through these curves must be the same, and corresponds to (28) with  $k = k^-$ . Therefore, it can be seen that  $F = 0$ ,  $\omega^{-1} = 3$ ,  $h = 9\pi/4$  and  $s_i = 7\pi/4 - \arcsin(1/\sqrt{5})$  is the solution of equation (31). Thus, using a suitable rescaling of the equations and change of variables and applying the Implicit Function Theorem as we did in Proposition 3.3, it is straightforward to prove that equations (31) define implicitly  $\sigma_2^-$  for  $\omega^{-1} - 3$  small enough. Finally, we have to recall that the Implicit Function Theorem, gives a curve for  $\omega^{-1}$  close to 3. Nevertheless, it only corresponds to a bifurcation curve for  $\omega^{-1} < 3$ , since  $\omega^{-1} > 3$  implies  $F > 0$  which does not have physical meaning.  $\square$

Expanding the variables of equation (31) in power series of  $\varepsilon = \omega^{-1} - 3$  for  $\varepsilon < 0$  as

$$\begin{cases} F = -\frac{3}{80}\pi\sqrt{5}\varepsilon + F_2\varepsilon^2 + F_3\varepsilon^3 + \mathcal{O}_4(\varepsilon) \\ h = \frac{9\pi}{4} + h_1\varepsilon + h_2\varepsilon^2 + h_3\varepsilon^3 + \mathcal{O}_4(\varepsilon) \\ s_i = \frac{7\pi}{4} - \arcsin \frac{1}{\sqrt{5}} + s_{i,1}\varepsilon + s_{i,2}\varepsilon^2 + s_{i,3}\varepsilon^3 + \mathcal{O}_4(\varepsilon) \text{ for } i = 1, 2. \end{cases}$$

one can obtain the local expansion of  $\sigma_2^-$ .

**Corollary 5.7.** *The local expansion of curve  $\sigma_2^-$  is given by*

$$\sigma_2^-(\varepsilon) = -\frac{3\pi\sqrt{5}}{80}\varepsilon + \left(\frac{1}{64} + \frac{57}{6400}\pi\right)\pi\sqrt{5}\varepsilon^2 - \frac{\pi\sqrt{5}}{2048000}\left(48089\pi^2\sqrt{2} + 14840\pi\sqrt{2} + 64800\pi^2 + 6240\sqrt{2}\right)\varepsilon^3 + \mathcal{O}(\varepsilon^4). \quad (32)$$

for  $\varepsilon < 0$ .

The computation for  $\sigma_2^+$  is analogous, but now the sliding motion starts in  $\partial\Sigma_c^+$  and ends in  $\partial\Sigma_c^-$ , and to first order  $h$  and  $s_i$  are given by  $h = 3\pi/4$  and  $s_i = 5\pi/4 + \arcsin(1/\sqrt{5})$ .

**Corollary 5.8.** *The local expansion of curve  $\sigma_2^+$  is given by*

$$\sigma_2^+(\varepsilon) = \frac{3\pi\sqrt{5}}{80}\varepsilon + \left(-\frac{1}{64} + \frac{21}{1280}\pi\right)\pi\sqrt{5}\varepsilon^2 + \left(\frac{39}{6400} - \frac{547}{25600}\pi + \frac{8581}{204800}\pi^2 - \frac{81}{2560}\pi^2\sqrt{2}\right)\pi\sqrt{5}\varepsilon^3 + \mathcal{O}(\varepsilon^4), \quad (33)$$

for  $\varepsilon > 0$ .

## 5.4 The crossing-sliding bifurcation curves $\sigma_3^\pm$

The curves  $\sigma_3^-$  and  $\sigma_3^+$  correspond to crossing-sliding bifurcations (see Figure 11). We explain the construction of the periodic orbit for parameters in  $\sigma_3^-$ . The situation for  $\sigma_3^+$  is similar. We let  $z_0 = (x_0, 0, s_0) \in \Sigma_c^-$  and  $z_1 = (-F + \sin(s_1), 0, s_1) \in \partial\Sigma_c^+$  for certain  $s_0$  and  $s_1$  the points where the periodic orbit hits  $\Sigma$ . Moreover, we consider  $(x^0(t), y^0(t), s^0(t))$  the backward trajectory with initial condition  $z_0$  and  $(x^1(t), y^1(t), s^1(t))$  and  $(x^2(t), y^2(t), s^2(t))$  the backward and forward trajectories with initial condition  $z_1 = (-F + \sin(s_1), 0, s_1)$ . Thus, in order to obtain the periodic orbit for parameters in  $\sigma_3^-$ , the following conditions must hold,

$$\begin{cases} x^1(-(s_1 - s_0)/\omega) = x_0 \\ y^1(-(s_1 - s_0)/\omega) = 0 \\ y^2(h) = 0 \\ y^0(h + (s_1 - s_0)/\omega - \pi/\omega) = 0 \\ x^2(h) + x^0(h + (s_1 - s_0)/\omega - \pi/\omega) = 0. \end{cases} \quad (34)$$

The first two equations guarantee that the trajectories  $(x^1(t), y^1(t), s^1(t))$  and  $(x^2(t), y^2(t), s^2(t))$  match at  $z_0$ , and the remainder that the limiting points of this half of the periodic orbit belong to  $\Sigma$  and are symmetric.

**Proposition 5.9.** *The crossing-sliding codimension-1 bifurcation curve  $\sigma_3^-$  emanating from  $B$  is defined implicitly for suitable values  $h, x_0, s_0$  and  $s_1$ , and for  $\omega^{-1} < 3$  close enough to  $\omega^{-1} = 3$  by equations (34).*

*Proof.* Proceeding as in the proof of Proposition 5.6, the limiting periodic orbit for parameters in  $\sigma_3^-$  tending to  $B$  is given by (28) with  $k = k^-$ . It can be seen that  $F = 0, \omega^{-1} = 3, h = 9\pi/4, x_0 = -3\sqrt{10}/10$  and  $s_i = 7\pi/4 - \arcsin(1/\sqrt{5})$  is solution of equation (34). Thus, using the suitable rescaling and change of variables and applying the Implicit Function Theorem as we did in Proposition 3.3, it is straightforward to prove that equations (31) define implicitly  $\sigma_3^-$  for  $\omega^{-1} - 3$  small enough. Nevertheless, it only corresponds to a bifurcation curve for  $\omega^{-1} < 3$ .  $\square$

Expanding the variables of equation (34) in power series of  $\varepsilon = \omega^{-1} - 3$  for  $\varepsilon < 0$  as

$$\begin{cases} F = -\frac{3}{80}\pi\sqrt{5}\varepsilon + F_2\varepsilon^2 + F_3\varepsilon^3 + \mathcal{O}_4(\varepsilon) \\ h = \frac{9\pi}{4} + h_1\varepsilon + h_2\varepsilon^2 + h_3\varepsilon^3 + \mathcal{O}_4(\varepsilon) \\ x_0 = -\frac{3\sqrt{10}}{10} + x_{0,1}\varepsilon + x_{0,2}\varepsilon^2 + x_{0,3}\varepsilon^3 + \mathcal{O}_4(\varepsilon) \\ s_i = \frac{7\pi}{4} - \arcsin\frac{1}{\sqrt{5}} + s_{i,1}\varepsilon + s_{i,2}\varepsilon^2 + s_{i,3}\varepsilon^3 + \mathcal{O}_4(\varepsilon) \text{ for } i = 1, 2. \end{cases}$$

one can obtain the local expansion of  $\sigma_3^-$ .

**Corollary 5.10.** *The local expansion of curve  $\sigma_3^-$  is given by*

$$\sigma_3^-(\varepsilon) = -\frac{3\pi\sqrt{5}}{80}\varepsilon + \frac{\pi\sqrt{5}}{64}(1 + 3\pi)\varepsilon^2 - \frac{\pi\sqrt{5}}{12800}\left(2187\pi^2\sqrt{2} + 874\pi + 7720\pi^2 + 78\right)\varepsilon^3 + \mathcal{O}(\varepsilon^4). \quad (35)$$

for  $\varepsilon < 0$ .

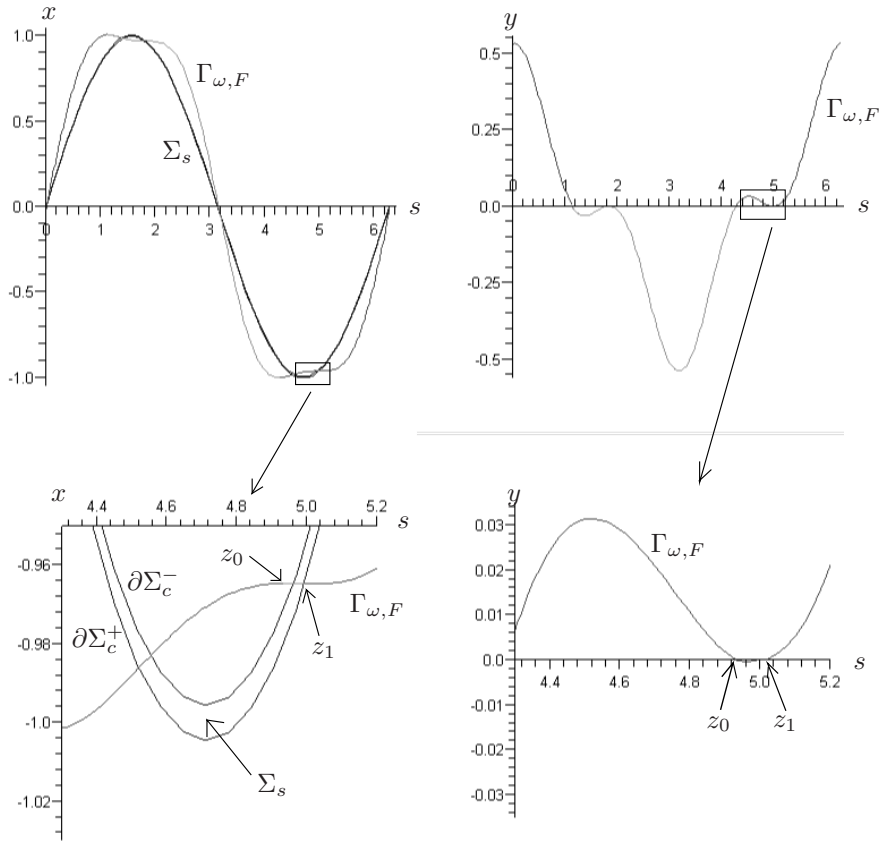


Figure 11: Projection of  $\Gamma_{\omega,F}$  onto the planes  $(s, x)$  and  $(s, y)$  for parameters in the curve  $\sigma_3^-$  are given in the upper pictures. A zoom of the rectangle around the fold point of the periodic orbit is given in the lower pictures. The points  $z_0$  and  $z_1$  are used in the construction of the periodic orbit. The first one belongs to the crossing region  $\Sigma_c^-$  and the second one to  $\partial\Sigma_c^+$ , and therefore is a fold point.

The study of  $\sigma_3^+$  is analogous, but now the tangency point belongs to  $\partial\Sigma_c^-$ , and at first order  $h$ ,  $x_0$  and  $s_i$  are given by  $h = 3\pi/4$ ,  $x_0 = -3\sqrt{10}/10$  and  $s_i = 5\pi/4 + \arcsin(1/\sqrt{5})$ .

**Corollary 5.11.** *The local expansion of curve  $\sigma_3^+$  is given by*

$$\sigma_3^+(\varepsilon) = \frac{3\pi\sqrt{5}}{80}\varepsilon + \pi\sqrt{5}\left(-\frac{1}{64} + \frac{87}{1600}\pi\right)\varepsilon^2 + \frac{\pi\sqrt{5}}{100}\left(\frac{39}{64} - \frac{481}{64}\pi + \frac{4663}{80}\pi^2 - \frac{2187}{128}\pi^2\sqrt{2}\right)\varepsilon^3 + \mathcal{O}(\varepsilon^4), \quad (36)$$

for  $\varepsilon > 0$ .

## 5.5 Comparison with previous numerical work

In Sections 5.2-5.4 we have obtained local expansions for the codimension-1 bifurcation curves which emanate from point  $B$ . We now can compare our analytical results with the numerical results obtained in [KP08]. In Figure 12 we plot the two sets of six curves and one can see that they fit very well close to

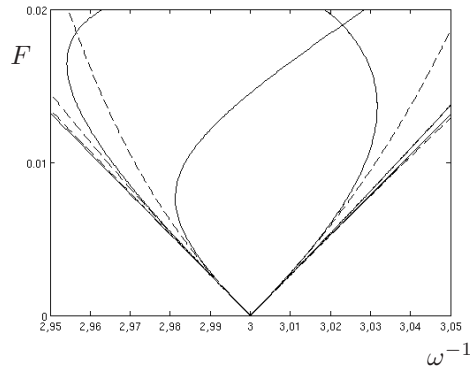


Figure 12: Comparison between the codimension-1 bifurcation curves emanating from  $B$  obtained numerically in [KP08] (continuous line) and the local expansions obtained in this article (dashed line).

the point  $B$ .

## 6 Conclusion

In this paper, we have studied analytically the two parameter bifurcation diagram of the friction oscillator with Coulomb friction. This model depends on two parameters and is a paradigm for Filippov systems. In certain range of these parameters the system has an attractor periodic orbit which undergoes a wide set of sliding bifurcations.

First, we have detected an infinite set of codimension-2 bifurcation points  $A_n$  which correspond to the periodic orbit cusp bifurcation. We have rigorously unfolded these bifurcations proving that from them emanate three codimension-1 bifurcation curves corresponding to crossing-sliding, grazing-sliding and switching-sliding bifurcations. For the first of these points,  $A_1 := (\omega^{-1}, F) = (2, 1/3)$ , we have computed the local expansions of these curves and found excellent agreement with the numerical results [KP08].

Second, we have considered the parameters for which the nonsmoothness disappears, which physically corresponds to the absence of friction. In that case we have seen that for most values of the frequency parameter, when we perturb the system, the nonsmooth obtained system mainly behaves as the smooth one, that is taking the friction to zero, the nonsmooth symmetric periodic orbit tends to the unique smooth symmetric periodic orbit. Nevertheless, for infinite (and discrete) values of the frequency for which all the smooth periodic orbits are symmetric, we obtain a second set of codimension-2 bifurcation points  $B_n$  around which seems to appear a very rich behaviour. We have focused our attention to the first of these points  $B_1 := (\omega^{-1}, F) = (3, 0)$ , and we have proved the existence of several codimension-1 bifurcation curves. We have also computed the local expansions of these curves, which show also excellent agreement with the numerical results in [KP08]. Around the other points  $B_n$  seems to exist more involved dynamics and, as far as the authors know, the possible bifurcations around them have not been studied even numerically.

## Acknowledgements

We wish to thank P. Kowalczyk and P. Piironen for making available their preprint [KP08] and for valuable discussions.

M. Guardia and T. M. Seara have been partially supported by the Spanish MCyT/FEDER grant MTM2006-00478 and S. J. Hogan by the UK EPSRC grant EP/E032249/1. In addition, the research of M. Guardia has been supported by the Spanish PhD grant FPU AP2005-1314. This work was initiated at the Research Semester “Non-Smooth Complex Systems” held at the CRM (Barcelona) in 2007.

## References

- [AS06] Viktor Avrutin and Michael Schanz. On multi-parametric bifurcations in a scalar piecewise-linear map. *Nonlinearity*, 19(3), 2006.
- [BG00] S. R. Bishop and U. Galvanetto. Dynamics of a simple damped oscillator undergoing stick-slip vibrations. *Meccanica*, (34):337–347, 2000.
- [BH03] B. B. Brogliato and W. P. M. H. Heemels. The complementarity class of hybrid dynamical systems. *Eur. J. Control*, (9):311–319, 2003.
- [BN99] C. J. Begely and Virgin L. N. Grazing bifurcations and basins of attraction in an impact-friction oscillator. *Physica D*, 130:43–57, 1999.
- [BPS01] Mireille E. Broucke, Charles C. Pugh, and Slobodan N. Simić. Structural stability of piecewise smooth systems. *Comput. Appl. Math.*, 20(1-2):51–89, 2001. The geometry of differential equations and dynamical systems.
- [BV01] S. Banerjee and G. C. Verghese. Nonlinear phenomena in power electronics: attractors, bifurcations, chaos, and nonlinear control. *IEEE Press*, 2001.
- [Cou85] C. A. Coulomb. Theorie des machines simples. *Memoires de Mathematique et de Physique de l’Academie des Sciences*, 10:161–331, 1785.
- [CS06] G. Csernák and G. Stépán. On the periodic response of a harmonically excited dry friction oscillator. *J. Sound Vibration*, 295(3-5):649–658, 2006.
- [CSS07] G. Csernák, G. Stépán, and S. W. Shaw. Sub-harmonic resonant solutions of a harmonically excited dry friction oscillator. *Nonlinear Dynam.*, 50(1-2):93–109, 2007.
- [Dan99] H. Dankowicz. On the modeling of dynamic friction phenomena. *Z. Angew. Math. Mech.*, 79(6):399–409, 1999.
- [dBBC08] M. di Bernardo, C. J. Budd, A. R. Champneys, and P. Kowalczyk. *Piecewise-smooth dynamical systems*, volume 163 of *Applied Mathematical Sciences*. Springer-Verlag London Ltd., London, 2008. Theory and applications.

- [dBKN03] M. di Bernardo, P. Kowalczyk, and A. Nordmark. Sliding bifurcations: a novel mechanism for the sudden onset of chaos in dry friction oscillators. *Internat. J. Bifur. Chaos Appl. Sci. Engrg.*, 13(10):2935–2948, 2003.
- [DK05] F. Dercole and Yu. A. Kuznetsov. Slidecont: An auto97 driver for sliding bifurcation analysis. *ACM Trans. Math. Softw.*, 31:95–119, 2005.
- [Fei94] M. I. Feigin. *Forced oscillations in systems with discontinuous nonlinearities*. Nauka, Moscow, 1994. In Russian.
- [FHS09] E. Fossas, S. J. Hogan, and T. M. Seara. Two-parameter bifurcation curves in power electronic converters. 19:341–357, 2009.
- [Fil88] A. F. Filippov. *Differential equations with discontinuous righthand sides*, volume 18 of *Mathematics and its Applications (Soviet Series)*. Kluwer Academic Publishers Group, Dordrecht, 1988.
- [FN97] Mats H. Fredriksson and Arne B. Nordmark. Bifurcations caused by grazing incidence in many degrees of freedom impact oscillators. *Proc. Roy. Soc. London Ser. A*, 453(1961):1261–1276, 1997.
- [Har31] J. P. Hartog. Forced vibrations with combined coulomb and viscous friction. *Transaction of the American Society of Mechanical Engineering*, 53:107–115, 1931.
- [JH] M.R. Jeffrey and S.J. Hogan. The geometry of generic sliding bifurcations. *SIAM Review*. submitted.
- [KdB05] P. Kowalczyk and M. di Bernardo. Two-parameter degenerate sliding bifurcations in Filippov systems. *Phys. D*, 204(3-4):204–229, 2005.
- [KdBC<sup>+</sup>06] P. Kowalczyk, M. di Bernardo, A. R. Champneys, S. J. Hogan, M. Homer, P. T. Piiroinen, Yu. A. Kuznetsov, and A. Nordmark. Two-parameter discontinuity-induced bifurcations of limit cycles: classification and open problems. *Internat. J. Bifur. Chaos Appl. Sci. Engrg.*, 16(3):601–629, 2006.
- [KP08] P. Kowalczyk and P. T. Piiroinen. Two-parameter sliding bifurcations of periodic solutions in a dry-friction oscillator. *Phys. D*, 237(8):1053–1073, 2008.
- [KRG03] Yu. A. Kuznetsov, S. Rinaldi, and A. Gragnani. One-parameter bifurcations in planar Filippov systems. *Internat. J. Bifur. Chaos Appl. Sci. Engrg.*, 13(8):2157–2188, 2003.
- [Kun00] M. Kunze. *Non-smooth dynamical systems*, volume 1744 of *Lecture Notes in Mathematics*. Springer-Verlag, Berlin, 2000.
- [NK06] A. B. Nordmark and P. Kowalczyk. A codimension-two scenario of sliding solutions in grazing-sliding bifurcations. *Nonlinearity*, 19, 2006.
- [Nor91] Arne B. Nordmark. Non-periodic motion caused by grazing incidence in impact oscillators. *J. Sound Vibration*, (2):279–297, 1991.

- [Nor02] Arne B. Nordmark. Discontinuity mappings for vector fields with higher order continuity. *Dyn. Syst.*, 17(4):359–376, 2002. Special issue: Non-smooth dynamical systems, theory and applications.
- [OHP95] M. Oestreich, N. Hinrichs, and K. Popp. Dynamical behaviour of friction oscillators with simultaneous self and external excitation. *Sadhana (Indian Academy of Sciences)*, 20:627–654, 1995.
- [SM07] D. J. W. Simpson and J. D. Meiss. Andronov-Hopf bifurcations in planar, piecewise-smooth, continuous flows. *Phys. Lett. A*, 371(3):213–220, 2007.
- [SM08] D. J. W. Simpson and J. D. Meiss. Neimark-Sacker bifurcations in planar, piecewise-smooth, continuous maps. *SIAM J. Appl. Dyn. Syst.*, 7(3):795–824, 2008.
- [SM09] D. J. W. Simpson and J. D. Meiss. Shrinking point bifurcations of resonance tongues for piecewise-smooth, continuous maps. *Nonlinearity*, 22(5):1123–1144, 2009.
- [Tei81] M. A. Teixeira. Generic singularities of discontinuous vector fields. *An. Acad. Brasil. Ciênc.*, 53(2), 1981.
- [Tei90] M. A. Teixeira. Stability conditions for discontinuous vector fields. *J. Differential Equations*, 88(1), 1990.
- [Tei93] M. A. Teixeira. Generic bifurcation of sliding vector fields. *J. Math. Anal. Appl.*, 176(2), 1993.
- [Tei99] M. A. Teixeira. Codimension two singularities of sliding vector fields. *Bull. Belg. Math. Soc. Simon Stevin*, 6(3), 1999.
- [Utk92] V. I. Utkin. *Sliding modes in control and optimization*. Communications and Control Engineering Series. Springer-Verlag, Berlin, 1992. Translated and revised from the 1981 Russian original.
- [WSWK08] J. Wojewoda, A. Stefański, M. Wiercigroch, and T. Kapitaniak. Hysteretic effects of dry friction: modelling and experimental studies. *Philos. Trans. R. Soc. Lond. Ser. A Math. Phys. Eng. Sci.*, 366(1866):747–765, 2008.